

# Recent Progress in Leptonic and Semileptonic Decays of Charmed Hadrons

Bai-Cian Ke\*

*Zhengzhou University, Zhengzhou 450001, People's Republic of China*

Jonna Koponen†

*PRISMA+ Cluster of Excellence & Institute for Nuclear Physics,  
Johannes Gutenberg University Mainz, Mainz, Germany, D-55128*

Hai-Bo Li‡

*Institute of High Energy Physics, Beijing 100049, People's Republic of China and  
University of Chinese Academy of Sciences, Beijing 100049, People's Republic of China*

Yangheng Zheng§

*University of Chinese Academy of Sciences, Beijing 100049, People's Republic of China*

We present a comprehensive review of purely leptonic and semileptonic decays of  $D^{0(+)}$ ,  $D_s^+$ , and charmed baryons (including  $\Lambda_c^+$ ,  $\Xi_c$  and  $\Omega_c$ ). The precise studies of these decays help deepen our understanding and knowledge of quantum chromodynamics via measuring decay constants and form factors, and test the Standard Model through examining the unitarity of Cabibbo-Kobayashi-Maskawa matrix and lepton flavor universality. We give an overview of the theoretical and experimental tools before discussing the recent progress. The data sets collected by BESIII near the production thresholds of  $D\bar{D}$ ,  $D_s^{(*)+}D_s^{(*)-}$  and  $\Lambda_c^+\bar{\Lambda}_c^-$  offer important opportunities for studies of charm physics.

arXiv:2310.05228v1 [hep-ex] 8 Oct 2023

---

\* baiciank@ihep.ac.cn

† jkoponen@uni-mainz.de

‡ lihb@ihep.ac.cn

§ zhengyh@ucas.edu.cn

## CONTENTS

I. Introduction	2
II. Theoretical framework: CKM matrix elements	3
III. Experimental overview	4
IV. Advantage of threshold production of charm hadron pairs	5
V. Lattice QCD overview	6
VI. Purely leptonic and semi-leptonic decays and lepton flavor universality	7
A. Leptonic decays and decay constants for $D^+$ and $D_s^+$	7
B. Semileptonic decays and transition form-factors	9
C. Discussion: $ V_{cd} $ and $ V_{cs} $ determinations	16
D. Lepton flavor universality	19
E. Rare leptonic and semileptonic $D_{(s)}$ decays	19
VII. Discussion and outlook	20
ACKNOWLEDGMENTS	21
References	22

## I. INTRODUCTION

The Standard Model (SM) is generally accepted as the theory of elementary particle interactions, with great success in describing a wide variety of experimental data with energies ranging from under a GeV up to a few TeV [1]. Quantum chromodynamics (QCD), the theory describing strong interaction in the SM, has been widely verified by experiments in the high energy region with its perturbation property, such as ATLAS, CMS, and LHCb experiments at the Large Hadron Collider (LHC). However, in the low energy region, the perturbative QCD is not applicable and faces huge challenges from both theory and experiment. The intriguing color nature of QCD also allows for the existence of gluon-rich matter, such as hybrids and glueballs, of which the unambiguous identification and understanding is clearly missing to date.

Furthermore, there are a number of unaddressed issues in the SM, which fails to explain many phenomena of nature. For example, a yet undiscovered source of  $CP$  violation in the quark sector could explain why matter dominates antimatter in the universe. We know from astrophysical observations that dark matter makes up most of the matter in the universe, and the existence of such a particle would have implications for the SM. Many of the BSM (beyond the SM) models addressing these questions could affect quark flavor interactions. Therefore, testing the SM is crucial, and the charm sector provides an excellent environment to do these tests.

Electron-positron  $e^+e^-$  colliders operating at the transition interval between non-perturbative QCD and perturbative QCD at a few GeV are uniquely well suited to play an important role in the understanding of strong interaction and precision test of the SM. Currently, the Beijing Spectrometer (BESIII) at the Beijing Electron-Positron Collider (BEPCII), with its unique features of threshold characteristics, quantum correlations, etc., has addressed a broad physics program covering tests of QCD, investigation of hadron spectroscopy, precision tests of electroweak interactions, and searches for new physics in low energy region.

On the theory side, lattice QCD (LQCD) provides a way to do QCD calculations non-perturbatively from first principles. Instead of approximating the QCD path integral by expanding it in a series in the strong coupling,  $\alpha_s$ , it can be calculated by discretizing the space-time. This reduces the path integral to have finite number of degrees of freedom, and imposes a natural regularization scheme for the theory. Instead of imposing an ultraviolet cutoff by hand, such as in Pauli-Villars regularization, waves with a wavelength smaller than  $\pi/a$ , where  $a$  is the lattice spacing, cannot exist in this discrete space, providing an automatic ultraviolet cutoff.

A typical LQCD simulation uses a space-time grid of  $64^3 \times 128$  or  $96^3 \times 192$ , i.e. the number of degrees of freedom is finite but quite large. These calculations become possible thanks to the computational power of modern supercomputers, and the utilization of advanced statistical techniques and Monte-Carlo integration. Regarding the achievable precision, the challenges are now different: while in a perturbative calculation the uncertainties come from the neglected higher order terms, in a LQCD calculation there is the statistical uncertainty from the Monte Carlo integration as well as systematic uncertainty from the discretization of the space-time. One needs to introduce a new dimensionful parameter, the lattice spacing  $a$ , and one has to extrapolate to continuum and infinite volume afterwards. The discretization is not unique, and it usually breaks some symmetries and introduces non-physical particles, whose contribution has to be suppressed. To some extent, one can choose which symmetries to preserve (at least partially) by choosing a suitable discretization scheme. A number of different discretization schemes have been developed and used over the years, and controlling and estimating the associated systematic uncertainties has been (and still is) the focus of modern LQCD calculations. The efforts have been successful, and LQCD has developed into a precision tool to do QCD calculations non-perturbatively from first principles to complement experiments.

In this review article, we give an overview of the theoretical and experimental tools, before discussing the recent progress in charmed hadron decays. Special attention is given to new results from BESIII. Charge-conjugated decay modes are implied throughout this review.

## II. THEORETICAL FRAMEWORK: CKM MATRIX ELEMENTS

The flavor-changing transition of quarks via interaction with a  $W^\pm$  boson is parameterized by the Cabibbo-Kobayashi-Maskawa (CKM) matrix [2], which is a  $3 \times 3$  unitary matrix:

$$V_{\text{CKM}} = \begin{pmatrix} V_{ud} & V_{us} & V_{ub} \\ V_{cd} & V_{cs} & V_{cb} \\ V_{td} & V_{ts} & V_{tb} \end{pmatrix}. \quad (1)$$

The CKM matrix elements represent the coupling strength through  $W^\pm$  boson weak interaction between up-type and down-type quarks. The diagonal elements, which describe transitions within the same generation, are measured to be of  $\mathcal{O}(1)$ , whereas the off-diagonal elements, which describe transitions among different generations, are of  $\mathcal{O}(10^{-2}-10^{-3})$ . In the case of charm physics, the  $c$  quark is more likely to decay to the  $s$  quark, called Cabibbo-favored, than to the  $d$  quark, called Cabibbo-suppressed.

The unitarity of  $V_{\text{CKM}}$  is a fundamental requirement of SM. Any deviation will reveal the sign of new physics. Consequently, a principal goal of flavor physics is to search evidence of the deviation with breakthrough in precision of the CKM matrix element measurements. The precision at which the elements in the first row,  $|V_{ud}|$  and  $|V_{us}|$ , are known has reached  $1 \times 10^{-4}-1 \times 10^{-3}$ , but that of the second row,  $|V_{cs}|$  and  $|V_{cd}|$ , is only  $\mathcal{O}(10^{-2})$  at present [1]. Improving the precision of the determination of the elements in the second row, therefore, will effectively enhance the sensitivity of testing the unitarity of CKM matrix. These elements in the charm sector,  $|V_{cs}|$  and  $|V_{cd}|$ , can be accessed by the purely leptonic and semi-leptonic charmed-meson decays. In a purely leptonic decay of a  $D_{(s)}^+$  meson, which is shown in the Feynman diagram in Fig. 1(a), the  $c$  quark and the  $d$  ( $s$ ) quark annihilate, followed by a weak

current connecting to the system of the lepton  $\ell^+$  and the corresponding flavored neutrino  $\nu_\ell$  ( $\ell = e, \mu, \tau$ ). The Feynman diagram in Fig. 1(b) depicts the semi-leptonic decay, where the initial-state charmed hadron evolves to the final-state hadrons along with a weak current emitted externally. Their decay rates are proportional to the product of the CKM matrix element  $|V_{cd(s)}|$  and the decay constant or form factors (see Eq. (6) in section VIA, and Eq. (10) in section VIB). Measurements of decay rates for the purely leptonic and semi-leptonic decays can be readily used to study weak-interaction physics.

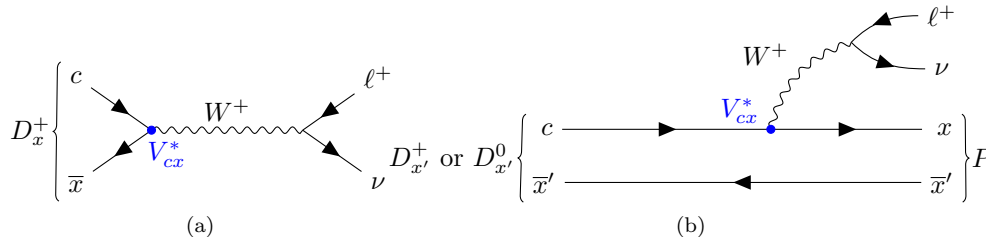


FIG. 1. Diagram of the purely leptonic (a) and semi-leptonic (b) decay of a  $D$  or  $D_s$  meson. Quark  $x$  is a  $d$  or an  $s$  quark, and  $x'$  is either  $u, d$  or  $s$ . The corresponding element of the CKM matrix,  $V_{cx}$ , appears in the vertex.

The CKM matrix can be parameterized by three mixing angles and one CP-violating complex phase [3]. The SM coupling strengths for the  $u - s$  and  $c - d$  transitions are both equal to  $G_F |\sin \theta_c|$  with a small, well understood,  $\mathcal{O}(10^{-4})$  correction. Here  $G_F$  is the Fermi constant, and  $\theta_c$ , one of the three mixing angles, is called the Cabibbo angle. Any significant difference in  $|\sin \theta_c|$  extracted from different quark transitions would be an unambiguous sign of new physics. The measured accuracy of about 0.2% level from nuclear  $\beta$  and kaon decays for  $|V_{ud}|$  and  $|V_{us}|$ , is more than an order of magnitude better than those from  $D_s$  and  $D$  decays for  $|V_{cs}|$  and  $|V_{cd}|$ , which is about 3%, based on statistics-limited BESIII measurements of  $D_s^+ \rightarrow \mu^+ \nu$ ,  $D^+ \rightarrow \mu^+ \nu$  and  $D^+ \rightarrow K^-(\pi^-) \ell^+ \nu_\ell$  decays. The clean environments for  $D^{+(0)}$  and  $D_s^+$  mesons produced by  $e^+e^- \rightarrow \psi(3770) \rightarrow D\bar{D}$  and  $\psi(4160) \rightarrow D_s^{*\pm} D_s^\mp$ , respectively, are especially well suited for low-systematic-uncertainty  $c$ -quark transition measurements. Year-long runs of future super tau-charm factory [4, 5] at  $\sqrt{s} = 3.773$  GeV and 4.160 GeV, which correspond to the rest masses of  $\psi(3770)$  and  $\psi(4160)$  respectively, would reduce the statistical uncertainties on  $c$ -quark-related determinations of  $|\sin \theta_c|$  to the level of about 0.2%, and match those from  $\beta$  and Kaon decays for the measurements of  $|V_{ud}|$  and  $|V_{us}|$ .

### III. EXPERIMENTAL OVERVIEW

Charmed hadrons can be produced at a range of different accelerators [6]. The production mechanisms are different, and the production cross-sections are largely varied.

The production cross-sections at hadron colliders are significantly higher than those at  $e^+e^-$  colliders. For example, the cross-section for producing  $c\bar{c}$  pairs in proton-proton collisions at the LHC with  $\sqrt{s} = 7$  TeV is more than a million times higher compared to operating an  $e^+e^-$  collider at the  $\psi(3770)$  and  $\Upsilon(4S)$  resonances of the charm and  $B$  factories [7–9]. For high energy hadron collisions, the fractional energy of the two colliding partons is likely to be different. This difference leads to an energy boost of the charmed hadrons of the collision system. Therefore, LHCb is ideally suited for performing decay-time dependent studies of charm decays. However, it is more difficult to study the leptonic and semileptonic decays of charmed hadrons at hadron colliders, as there are fewer kinematic constraints.

At  $e^+e^-$  colliders, there are more kinematic constraints available since the collision energy of the initial electron and positron is well known. The trigger efficiency of hadronic events at  $e^+e^-$  colliders can reach almost 100%, and with a relatively clean environment compared to hadron colliders. Two different running conditions can be operated for studying the charm physics. Running at a higher  $\sqrt{s}$  to produce  $\Upsilon(4S)$  on resonance is used by the  $B$  factories: BaBar and Belle/Belle II experiments, which are located at the PEP-II and KEKB/Super KEKB colliders, respectively. Both PEP-II and KEKB/Super KEKB are asymmetric colliders, which means that the energies of the  $e^+$  and  $e^-$  beams differ. Hence, they have a collision system that is boosted with respect to the laboratory frame. This allows decay-time dependent studies for charmed hadrons. The alternative is tuning  $\sqrt{s}$  to slightly more than the production threshold of charmed (anti-charmed) hadron pairs. Since there is no extra energy for producing pions, the decay goes almost exclusively through charmed hadron pairs. This production mode has been used for the CLEO-c experiment at the

CESR-c collider as well as for BESIII at BEPCII, which is ideally suited for the studies of leptonic and semileptonic decays of charmed hadrons. However, it is worth mentioning that the decay-time dependent studies of charmed hadrons are not possible for these experiments since the collisions happen at rest.

BESIII has collected data samples with integrated luminosity of  $8.0 \text{ fb}^{-1}$  at center-of-mass energy ( $\sqrt{s}$ )  $3.773 \text{ GeV}$ ,  $7.33 \text{ fb}^{-1}$  at  $\sqrt{s} = 4.128\text{-}4.226 \text{ GeV}$ , and  $4.5 \text{ fb}^{-1}$  between  $\sqrt{s} = 4.600$  and  $4.699 \text{ GeV}$ ; these  $\sqrt{s}$  values are optimal for the accumulation of  $D\bar{D}$ ,  $D_s^{*+}D_s^-$ , and  $\Lambda_c^+\bar{\Lambda}_c^-$  events near thresholds, respectively. BESIII will ultimately collect data samples with integrated luminosities of  $20 \text{ fb}^{-1}$  at  $\sqrt{s} = 3.773 \text{ GeV}$  and  $6 \text{ fb}^{-1}$  around  $4.18 \text{ GeV}$  in the near future. The kinematics at threshold allows the undetected neutrinos to be reconstructed according to the four-momentum conservation. Charmed hadron (semi-)leptonic measurements with these data samples provide rigorous tests of QCD, CKM unitarity, and lepton flavor universality (LFU) that complement similar studies of beauty hadrons. For charmed baryons, the measurement of the branching fraction of  $\Lambda_c^+ \rightarrow \Lambda \ell^+ \nu_\ell$  was first performed by the ARGUS collaboration [10] and subsequently by the CLEO collaboration [11]. Recently, the BESIII Collaboration measured the absolute branching fraction of  $\Lambda_c^+ \rightarrow \Lambda \ell^+ \nu_\ell$  [12, 13]. In addition to precision branching fractions of the  $\Lambda_c$ , if the BEPCII c.m. energy were upgraded to reach above  $4.95 \text{ GeV}$ , slightly beyond the current plan of  $4.9 \text{ GeV}$ , pairs of  $\Sigma_c$  and  $\Xi_c$  baryons could also be produced and studied.

BEPCII delivered its first physics data set in 2009 on the  $\psi(2S)$  peak. Since then, BESIII has collected more than  $40 \text{ fb}^{-1}$  of integrated luminosity at different  $\sqrt{s}$  from  $2.0$  to  $4.95 \text{ GeV}$ . In order to extend the physics potential of the BESIII experiment, two upgrade plans for BEPCII were proposed and approved in 2020. The first upgrade will increase the maximum beam energy to  $2.8 \text{ GeV}$  (corresponding to  $\sqrt{s} = 5.6 \text{ GeV}$ ), which will expand the energy reach of the collider into new territory. The second upgrade will increase the peak luminosity by a factor of 3 for  $\sqrt{s} = 4.0\text{-}5.6 \text{ GeV}$ . It will take about 2.5 years to prepare the upgraded components and half a year for installation and commissioning, which will start in June 2024 and finish in December 2024. With these upgrades, BESIII will enhance its capabilities to explore physics of the exotic charmonium-like states (XYZ) and will have the unique ability to perform precision measurements of the production and decays of charmed mesons and baryons at different thresholds. Recently, two  $e^+e^-$  collider experiments are proposed in Russia (SCTF) and China (STCF), which will act as super Charm factories [4, 5] with much improved luminosity and broader energy range for BESIII experiment.

#### IV. ADVANTAGE OF THRESHOLD PRODUCTION OF CHARM HADRON PAIRS

The neutrinos produced in (semi-)leptonic processes cannot be directly detected. However, the kinematics of threshold production of the charmed hadron pairs allow a tag technique to be employed, which provides a unique, low-background environment to measure the absolute branching fractions for charmed hadrons decaying to leptonic and semi-leptonic final states although it contains one undetectable particle.

The  $\psi(3770)$  resonance is predominantly decays to final states with a  $D\bar{D}$  meson pair ( $D\bar{D}$  represents  $D^+D^-$  or  $D^0\bar{D}^0$ ). The leftover phase-space is only  $30\text{-}40 \text{ MeV}/c^2$ , which is not even enough for the lightest hadron,  $\pi$ . Hence, when a  $D$  (or  $\bar{D}$ ) meson is reconstructed via one of its hadronic decay modes, the other  $\bar{D}$  (or  $D$ ) must be the parent of all the remaining particles in the event, even if some of them escape from the detector. In the case of (semi-)leptonic decays, the mass of the missing neutrino can be inferred from the four-momentum conservation. This tagging feature is a robust tool for charmed particle decay measurements in near threshold experiments.

There are two types of samples used in the tag technique: single tag (ST) and double tag (DT). In the ST sample, a charmed hadron (such as a  $D$  meson) is reconstructed through a particular hadronic decay without any requirement on the remaining reconstructed particle candidates. To select or extract the signal yields of the ST sample, beam constrained mass  $M_{BC}$  and energy difference  $\Delta E$  are the variables usually used:

$$M_{BC} = \sqrt{E_{\text{beam}}^2 - |\vec{p}_D|^2}, \quad \Delta E = E_D - E_{\text{beam}}, \quad (2)$$

where  $|\vec{p}_D|$  and  $E_D$  are the total reconstructed momentum and energy of the  $D$  candidate in the center-of-mass frame of the  $\psi(3770)$  resonance, respectively, and  $E_{\text{beam}}$  is the calibrated beam energy. The  $D$  signals will be consistent with the nominal  $D$  mass in  $M_{BC}$  and with  $\Delta E = 0$ .

In the DT sample, events can be fully reconstructed. The  $D$  hadron of the pair, designated as the ‘‘tag’’ side, is usually reconstructed through well-measured hadronic decay channels, while the anti- $D$ -hadron of the pair, designated

as the “signal” side, can be reconstructed through the (semi-)leptonic decay mode of interest. The information of the undetectable particle, e.g. neutrinos, are accessed via the missing four-momentum.

The yield of a ST sample of a tag mode is given by

$$N_{\text{tag}}^{\text{ST}} = 2N_{D\bar{D}}\mathcal{B}_{\text{tag}}\varepsilon_{\text{tag}}, \quad (3)$$

and the yield of a DT sample is given by

$$N_{\text{tag,sig}}^{\text{DT}} = 2N_{D\bar{D}}\mathcal{B}_{\text{tag}}\mathcal{B}_{\text{sig}}\varepsilon_{\text{tag,sig}}, \quad (4)$$

where  $N_{D\bar{D}}$  is the total number of produced  $D\bar{D}$  pairs,  $\mathcal{B}_{\text{tag(sig)}}$  is the branching fraction of the tag (signal) side, and the  $\varepsilon$  are the corresponding efficiencies. The branching fraction of the signal decay under study can be determined by isolating  $\mathcal{B}_{\text{sig}}$  such that

$$\mathcal{B}_{\text{sig}} = \frac{N_{\text{tag,sig}}^{\text{DT}}}{N_{\text{tag}}^{\text{ST}}} \frac{\varepsilon_{\text{tag}}}{\varepsilon_{\text{tag,sig}}}. \quad (5)$$

Another advantage of the tag technique is that the efficiency for reconstructing the tag-side should almost cancel and any residual effects caused by the tag-side are expected to be negligible since the efficiency approximately factorizes:  $\varepsilon_{\text{tag,sig}} \approx \varepsilon_{\text{tag}}\varepsilon_{\text{sig}}$ . The residual effects might occur when the factorization is violated. In other words, the DT efficiency is not completely the product of both sides’ ST efficiencies, since ST candidates are measured with the other  $D$  hadron of the pair decaying generically, while the tag side of DT candidates are measured versus a specific decay mode. The numbers and types of the decay products of the other  $D$  hadron matters due to overlapping on the detector. This effect, however, is believed to be small due to the fine-grained BESIII detector.<sup>1</sup>

The  $D_s^+$  samples are mainly obtained from the dataset at  $\sqrt{s} = 4.128\text{--}4.226$  GeV through the process  $e^+e^- \rightarrow D_s^{*\pm}D_s^\mp \rightarrow \gamma/\pi^0 D_s^+ D_s^-$ .<sup>2</sup> Unlike  $D\bar{D}$  pairs,  $D_s^+ D_s^-$  pairs don’t evenly share the four-momentum of the  $e^+e^-$  system. Accordingly, the recoil mass of the tag  $D_s$  is a popular variable to select signal events while the tag technique is still a robust tool.

## V. LATTICE QCD OVERVIEW

Given experimental measurements of the branching fractions of charmed hadron decays, combined with sufficiently precise theoretical calculations of the hadronic matrix elements, together they enable the determination of the CKM matrix elements  $|V_{cd}|$  and  $|V_{cs}|$  and a precise test of the unitarity of the second row of the CKM matrix. Significant progress has been made in charm physics on the lattice in recent years, largely due to the availability of gauge configurations produced using highly-improved lattice-fermion actions that enable treating the  $c$  quark with the same action as for the  $u$ ,  $d$ , and  $s$  quarks. Different LQCD collaborations use different discretizations of the gluon and fermion actions, which is important for cross-checks to uncover potential systematic effects. The analysis techniques used by different groups may also differ, and the results should only agree after the physical/continuum limit has been taken. Indeed, the consistency of values obtained using different formulations adds significantly to our confidence in the results.

In this review we use lattice results reported by the Flavour Lattice Averaging Group (FLAG) in their 2021 review (published in 2022) [14]. FLAG has a set of guidelines to combine current, published LQCD results, including only lattice calculations for which all systematic effects have been taken into account, into a world average. In some cases only a single result enters the average, but more often it is a combination of results from different collaborations. The lattice results are grouped and listed according to the number of sea-quark flavors used in the calculation. Here we take the  $n_f = 2+1+1$  results, that include  $u/d$ ,  $s$  and  $c$  quarks in the sea, if these results are available — otherwise

<sup>1</sup> The violations of factorization are not negligible, but the effect is taken into account in the Monte-Carlo simulation. In practice, the systematic uncertainty caused by tag sides is about 0.1%.

<sup>2</sup> The threshold of  $D_s^\pm D_s^\mp$  pairs is at about  $\sqrt{s} = 4.009$  GeV, while the cross section is only about one third of that for  $e^+e^- \rightarrow D_s^{*\pm} D_s^\mp$  at  $\sqrt{s} = 4.180$  GeV.

we take the  $n_f = 2 + 1$  results. The 2 here means that  $u$  and  $d$  quarks are treated as degenerate on the lattice, which helps in keeping the computational cost of the calculations reasonable. For charm decays, this is estimated to be a small effect and can be taken into account. Calculations that include  $n_f = 1 + 1 + 1 + 1$  flavors of sea quarks, treating  $u$  and  $d$  quarks as non-degenerate, are now emerging for quantities where the effect is expected to be most important.

## VI. PURELY LEPTONIC AND SEMI-LEPTONIC DECAYS AND LEPTON FLAVOR UNIVERSALITY

One of the most charming feature of charmed mesons is that their  $\sim 2$  GeV masses locate them in the region where nonperturbative QCD is activated. This fact is an obstacle to study their hadronic transitions, but their purely leptonic and semi-leptonic decays play an important medium to facilitate such investigation. Purely leptonic and semi-leptonic decays of  $D_{(s)}^+$  provide the cleanest and best access to understand the mechanism of the  $c$  quark to the  $d(s)$  quark transition (Fig. 1). In both decays, because strong interactions affect only the hadronic system, the weak and strong interactions can be well separated allowing the most precise determinations of corresponding decay constants (Sec. VIA), form factors (Sec. VIB), and CKM matrix elements (Secs. II and VIC).

### A. Leptonic decays and decay constants for $D^+$ and $D_s^+$

The leptonic decay of the charmed meson  $D_{(s)}^+$  could happen by the annihilation of the  $c$  and  $\bar{d}(\bar{s})$  quarks into  $\ell^+\nu_\ell$  mediated by a virtual  $W^+$  boson. The partial decay width of the  $D_{(s)}^+ \rightarrow \ell^+\nu_\ell$  to the lowest order within SM, due to the isolation of the weak and strong effects, is proportional to the product of the decay constant  $f_{D_{(s)}^+}$  (parametrizing strong-interaction effects between the two initial-state quarks) and the CKM matrix element  $|V_{cd(s)}|$  (parametrizing the  $c \rightarrow s(d)$  flavor-changing interaction), given in a simple form: [15]

$$\Gamma(D_{(s)}^+ \rightarrow \ell^+\nu_\ell) = \frac{G_F^2 f_{D_{(s)}^+}^2}{8\pi} |V_{cd(s)}|^2 m_\ell^2 M_{D_{(s)}^+} \left(1 - \frac{m_\ell^2}{M_{D_{(s)}^+}^2}\right)^2, \quad (6)$$

where  $m_\ell$  and  $M_{D_{(s)}^+}$  stand for the  $\ell$  lepton and the  $D_{(s)}^+$  meson invariant mass, respectively. The partial decay width is calculated by the branching fraction (Eq. 5) divided by the  $D_{(s)}^+$  life time obtained through global fit [1]. The decay constants  $f_{D_{(s)}^+}$  can be calculated using LQCD, while the CKM matrix elements can only be determined by experimental measurements. Measuring the partial decay width (or branching fraction) of  $D_{(s)}^+ \rightarrow \ell^+\nu_\ell$ , one can either determine the  $f_{D_{(s)}^+}$  by taking the  $|V_{cd(s)}|$  from the SM global fit [16], or extract the  $|V_{cd(s)}|$  with the help of the  $f_{D_{(s)}^+}$  predicted by LQCD. The precision of the  $f_{D_{(s)}^+}$  or  $|V_{cd(s)}|$  determination is directly propagated from the precision of the  $D_{(s)}^+ \rightarrow \ell^+\nu_\ell$  measurement, since the uncertainties associated with the higher-order correction of the SM model and the precisely measured  $G_F$ ,  $m_\ell$  and  $M_{D_{(s)}^+}$  are negligible with current statistics.

In LQCD calculations, the decay constants  $f_{D_{(s)}^+}$  are extracted from Euclidean matrix elements of the axial current

$$\langle 0 | A_{cx}^\mu | D_x(p) \rangle = i f_{D_x} p^\mu, \quad (7)$$

with  $x = d$  or  $s$  quark,  $A_{cx}^\mu = \bar{c} \gamma_\mu \gamma_5 x$  and  $p$  momentum of the  $D_x$  meson. Results for  $n_f = 2 + 1 + 1$  dynamical flavors from the FLAG review [14] are summarized in Table I alongside experimental results. In the case of LQCD, we list isospin-averaged quantities, although, in a few cases, results for  $f_{D^+}$  have been published [17–19]. In one of the lattice calculations, the difference between  $f_D$  and  $f_{D^+}$  has been estimated to be  $0.58 \pm 0.07$  MeV [19]. The results for the decay constants from LQCD are very precise, the total uncertainties (including both statistical and systematic uncertainties) for the FLAG averages being 0.33% and 0.2% for  $f_D$  and  $f_{D_s}$ , respectively.

In recent years, the BESIII collaboration has reported the most precise experimental studies of  $D_{(s)}^+ \rightarrow \ell^+\nu_\ell$  by using  $e^+e^-$  annihilation data corresponding to a total integrated luminosity of 2.93, 0.48, and 6.32 fb $^{-1}$  collected at  $\sqrt{s} = 3.773$  GeV for  $D^0\bar{D}^0/D^+D^-$ , 4.009 GeV for  $D_s^+D_s^-$ , and 4.178-4.226 GeV for  $D_s^{*\pm}D_s^\mp$ , respectively [20, 22–26].

TABLE I. Measurements of  $D^+$  and  $D_s^+$  purely leptonic decays with threshold data at BESIII, and comparisons between experimental results and theoretical expectation or SM-global fit results. (Here, “-” indicates not available.) For theory predictions of the decay constants, we take the Flavour Lattice Averaging Group (FLAG) averages [14] of calculations with  $n_f = 2 + 1 + 1$  sea quarks. The original calculations included in the average are cited next to the results. Note that these predictions, which are marked with an asterisk in the table, are for the isospin-averaged quantities  $f_D$  and  $f_{D_s}$ . In a few cases, results for  $f_{D^+}$  have been published [17–19], and the difference between  $f_D$  and  $f_{D^+}$  has been estimated to be  $0.58 \pm 0.07$  MeV [19]. We add this to the isospin-averaged quantity and combine the lattice estimate for  $f_D$  with the experimental result for  $f_{D^+}|V_{cd}|$  to get an estimate for the CKM element given in the “Measurement” column. For  $f_{D_s}$  we assume the difference between  $f_{D_s}$  and  $f_{D_s^+}$  is the same 0.58 MeV, but double the uncertainty to be conservative in estimating the uncertainty. The values given for  $V_{cs}$  in the “Measurement” column are then calculated from the experimental result for  $f_{D_s^+}|V_{cs}|$  and the LQCD result for the decay constant. For comparison, we give the values of the CKM elements extracted by the CKMfitter group [16] in the “Prediction/Fit” column.

Observable	Measurement	Prediction/Fit
$\mathcal{B}(D^+ \rightarrow \mu^+ \nu_\mu)$	$(3.71 \pm 0.19_{\text{stat}} \pm 0.06_{\text{syst}}) \times 10^{-4}$ [20]	-
$f_{D^+} V_{cd} $	$(45.75 \pm 1.20_{\text{stat}} \pm 0.39_{\text{syst}})$ MeV	-
$f_{D^+}$	$(203.8 \pm 5.2_{\text{stat}} \pm 1.8_{\text{syst}})$ MeV	$(212.0 \pm 0.7)$ MeV* [19, 21]
$ V_{cd} $	$0.2152 \pm 0.0060$	$0.22487^{+0.00024}_{-0.00021}$
$\mathcal{B}(D^+ \rightarrow \tau^+(\pi^+\bar{\nu}_\tau)\nu_\tau)$	$(1.20 \pm 0.24_{\text{stat}} \pm 0.12_{\text{syst}}) \times 10^{-3}$ [22]	-
$\Gamma(D^+ \rightarrow \tau^+\nu_\tau)/\Gamma(D^+ \rightarrow \mu^+\nu_\mu)$	$3.21 \pm 0.74$ [22]	2.67
$\mathcal{B}(D_s^+ \rightarrow \mu^+ \nu_\mu)$	$(5.35 \pm 0.13_{\text{stat}} \pm 0.16_{\text{syst}}) \times 10^{-3}$ [23]	-
$f_{D_s^+} V_{cs} $	$(243.1 \pm 3.0_{\text{stat}} \pm 3.7_{\text{syst}})$ MeV	-
$f_{D_s^+}$	$(249.8 \pm 3.0_{\text{stat}} \pm 3.8_{\text{syst}})$ MeV	$(249.9 \pm 0.5)$ MeV* [19, 21]
$ V_{cs} $	$0.971 \pm 0.019$	$0.973521^{+0.000057}_{-0.000062}$
$\mathcal{B}(D_s^+ \rightarrow \tau^+(\pi^+\bar{\nu}_\tau)\nu_\tau)$	$(5.22 \pm 0.25_{\text{stat}} \pm 0.17_{\text{syst}})\%$ [23]	-
$f_{D_s^+} V_{cs} $	$(243.0 \pm 5.8_{\text{stat}} \pm 4.0_{\text{syst}})$ MeV	-
$f_{D_s^+}$	$(249.7 \pm 6.0_{\text{stat}} \pm 4.2_{\text{syst}})$ MeV	$(249.9 \pm 0.5)$ MeV* [19, 21]
$ V_{cs} $	$0.970 \pm 0.028$	$0.973521^{+0.000057}_{-0.000062}$
$\mathcal{B}(D_s^+ \rightarrow \tau^+(\rho^+\bar{\nu}_\tau)\nu_\tau)$	$(5.29 \pm 0.25_{\text{stat}} \pm 0.20_{\text{syst}})\%$ [24]	-
$f_{D_s^+} V_{cs} $	$(244.8 \pm 5.8_{\text{stat}} \pm 4.8_{\text{syst}})$ MeV	-
$f_{D_s^+}$	$(251.6 \pm 5.9_{\text{stat}} \pm 4.9_{\text{syst}})$ MeV	$(249.9 \pm 0.5)$ MeV* [19, 21]
$ V_{cs} $	$0.977 \pm 0.030$	$0.973521^{+0.000057}_{-0.000062}$
$\mathcal{B}(D_s^+ \rightarrow \tau^+(e^+\nu_e\bar{\nu}_\tau)\nu_\tau)$	$(5.27 \pm 0.10_{\text{stat}} \pm 0.12_{\text{syst}})\%$ [25]	-
$f_{D_s^+} V_{cs} $	$(244.4 \pm 2.3_{\text{stat}} \pm 2.9_{\text{syst}})$ MeV	-
$f_{D_s^+}$	$(251.1 \pm 2.4_{\text{stat}} \pm 3.0_{\text{syst}})$ MeV	$(249.9 \pm 0.5)$ MeV* [19, 21]
$ V_{cs} $	$0.976 \pm 0.015$	$0.973521^{+0.000057}_{-0.000062}$
$\Gamma(D_s^+ \rightarrow \tau^+\nu_\tau)/\Gamma(D_s^+ \rightarrow \mu^+\nu_\mu)$	$9.80 \pm 0.34$ [1]	9.75

With the 3.773 GeV data sample, BESIII measured the branching fraction of  $D^+ \rightarrow \mu^+\nu_\mu$  [20], and either used lattice results on the decay constant  $f_{D^+}$  to extract the CKM matrix element  $|V_{cd}|$  or used global fit of  $|V_{cd}|$  to obtain  $f_{D^+}$ . Furthermore, BESIII observed the  $D^+ \rightarrow \tau^+(\pi^+\bar{\nu}_\tau)\nu_\tau$  decay for the first time [22]. The corresponding results are summarized in Table I. A total of about 1.7 million  $D^-$  events are tagged through nine  $D^-$  hadronic decays (summing up to 30% of all  $D^-$  decays). Signal candidates of  $D^+ \rightarrow \mu^+\nu_\mu$  or  $D^+ \rightarrow \tau^+(\pi^+\bar{\nu}_\tau)\nu_\tau$  are then reconstructed recoiling against the tagged  $D^-$  mesons by requiring exactly one track identified as  $\mu^+$  or  $\pi^+$ .<sup>3</sup> The neutrino is undetectable, but the yields of the signal decays can be extracted from the missing-mass-squared variable  $\text{MM}^2 = (E_{\text{beam}} - E_{\mu/\pi})^2 - (-\vec{p}_{\text{tag}} - \vec{p}_{\mu/\pi})^2$ , where  $E_{\mu/\pi}$  and  $\vec{p}_{\mu/\pi}$  ( $\vec{p}_{\text{tag}}$ ) are the energy and three-momentum of the reconstructed  $\mu^+$  or  $\pi^+$  (tagged  $D^-$  mesons). The  $D^+ \rightarrow \mu^+\nu_\mu$  signal events have only one neutrino missing and peak around  $\text{MM}^2 = 0$ , which represents the negligible invariant mass of neutrinos. In the case of  $D^+ \rightarrow \tau^+(\pi^+\bar{\nu}_\tau)\nu_\tau$ , the two missing neutrinos push the signal distribution toward  $\text{MM}^2 > 0$  and lead to a more complex background than that in the  $D^+ \rightarrow \mu^+\nu_\mu$  decay.

<sup>3</sup> The electron final state  $D^+ \rightarrow e^+\nu_e$  is suppressed due to helicity suppression.



With the 4.178-4.226 GeV data samples, BESIII studied the  $D_s^+ \rightarrow \mu^+ \nu_\mu$  [23, 26] and  $D_s^+ \rightarrow \tau^+ \nu_\tau$  decays with three  $\tau^+$  decays:  $\rho^+ \bar{\nu}_\tau$  [24],  $\pi^+ \bar{\nu}_\tau$  [23], and  $e^+ \nu_e \bar{\nu}_\tau$  [25]. The measured branching fractions, decay constant  $f_{D_s^+}$  and CKM matrix element  $|V_{cs}|$  are listed in Table I. Using a similar method as for the  $D^+$  purely leptonic decays, the  $D_s^+ \rightarrow \mu^+ \nu_\mu$  (Fig. 2(a)),  $D_s^+ \rightarrow \tau^+(\pi^+ \bar{\nu}_\tau) \nu_\tau$ , and  $D_s^+ \rightarrow \tau^+(\rho^+ \bar{\nu}_\tau) \nu_\tau$  signal yields are obtained from the  $MM^2$  distributions. However,  $D_s^+ \rightarrow \tau^+(e^+ \nu_e \bar{\nu}_\tau) \nu_\tau$  has three neutrinos missing, degrading  $MM^2$  into a non-ideal place to extract signal yields. Instead, the total energy of extra photons not used in event selection ( $E_{\text{extra}}^{\text{tot}}$ ) is employed to extract  $D_s^+ \rightarrow \tau^+(e^+ \nu_e \bar{\nu}_\tau) \nu_\tau$  signal yields (Fig. 2(b)). Different decay processes cause different numbers and energies of real/fake photons inside the detector, and this decay causes a very distinct peak at low  $E_{\text{extra}}^{\text{tot}}$  where the backgrounds are small.

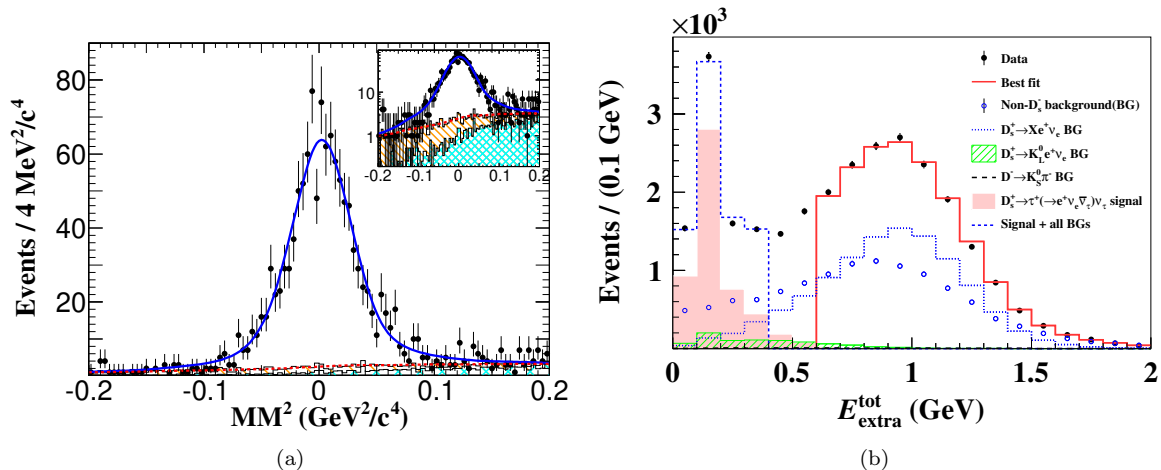


FIG. 2. (a) The squared missing mass ( $MM^2$ ) distribution of the selected  $D_s^+ \rightarrow \mu^+ \nu_\mu$  candidates from Ref. [26]. The error bars show the statistical uncertainty in experimental data. The inset shows the same distribution in logarithmic scale. Panel from Ref. [26]. (b) The  $E_{\text{extra}}^{\text{tot}}$  distribution of the selected  $D_s^+ \rightarrow \tau^+(e^+ \nu_e \bar{\nu}_\tau) \nu_\tau$  candidates from Ref. [25]. The backgrounds, including non- $D_s^-$ ,  $D_s^+ \rightarrow K_L^0 e^+ \nu_e$ , and  $D_s^+ \rightarrow X e^+ \nu_e$ , are estimated by a fit to the region  $E_{\text{extra}}^{\text{tot}} > 0.6$  GeV and extrapolated into the signal region  $E_{\text{extra}}^{\text{tot}} < 0.4$  GeV using Monte-Carlo simulated shapes. Panel from Ref. [25].

The most precise measured  $f_{D^+} |V_{cd}|$  value can be obtained via the  $D^+ \rightarrow \mu^+ \nu_\mu$  decay. The  $D^+ \rightarrow \tau^+(\pi^+ \bar{\nu}_\tau) \nu_\tau$  contributes very little due to its large uncertainty. The most precise measurement of  $f_{D_s^+} |V_{cs}|$  comes from the  $D_s^+$  purely leptonic decays. In this case,  $D_s^+ \rightarrow \mu^+ \nu_\mu$  and  $D_s^+ \rightarrow \tau^+ \nu_\tau$  make comparable contributions (listed in Table I). Along with the values of  $|V_{cd}|$  and  $|V_{cs}|$  from the SM-constrained fit [1],  $f_{D^+}$  and  $f_{D_s^+}$  can be extracted. The comparisons of various measurements are shown in Fig. 3. Furthermore, the Heavy Flavor Averaging Group (HFLAV) [27], having the measured  $f_{D_s^+} |V_{cs}|$  and  $f_{D^+} |V_{cd}|$ , gives a value  $f_{D_s^+} / f_{D^+} = 1.232 \pm 0.030$ , which is roughly  $1.8\sigma$  higher than the lattice value from the FLAG world average value,  $1.1783 \pm 0.0016$  [14].

## B. Semileptonic decays and transition form-factors

In the SM, the theoretical description of semileptonic decays involve a leptonic current along with a hadronic current. The effects of these two currents can be well-isolated [39] since the leptonic and hadronic systems have no strong interactions between their final-states. The hadronic current in the charm physics region is non-perturbative, and the hadronic matrix element is thus well suited for a LQCD calculation.

The simplest case of the semi-leptonic  $D_{(s)}^{0(+)}$  decays is  $D^{0/+} \rightarrow P \ell^+ \nu_\ell$  (where  $P$  denotes a pseudoscalar meson).

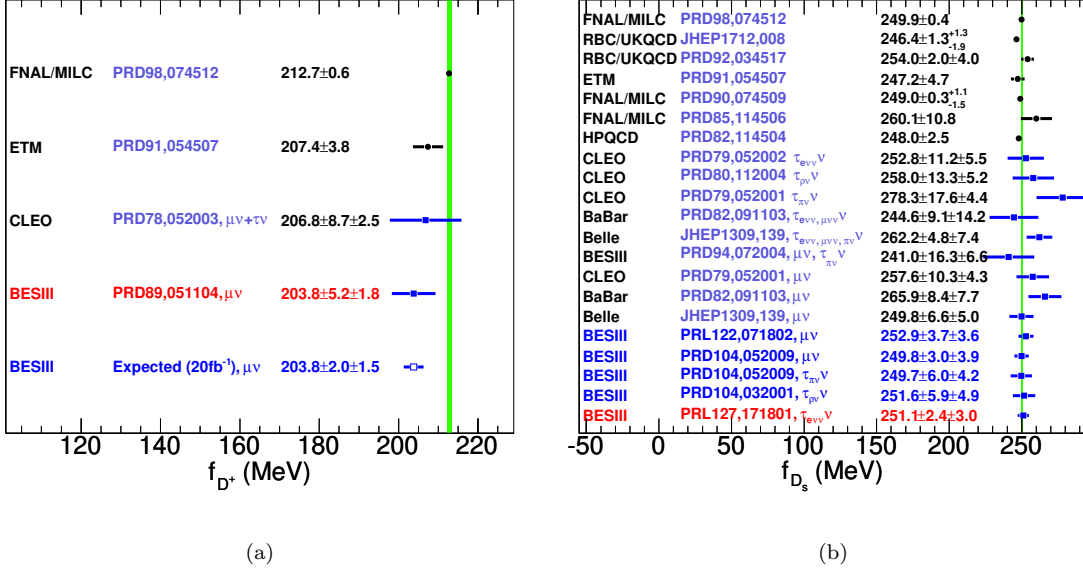


FIG. 3. Comparison of the results for (a)  $f_{D^+}$  and (b)  $f_{D_s^+}$  measured by the BESIII, Belle, BaBar, and CLEO experiments. The green bands present the LQCD uncertainties. Values marked in black circle denote LQCD calculations, values marked in blue square denotes experimental results, and the value marked in open square denotes the expected precision from BESIII with 20 fb<sup>-1</sup> data set at 3.773 GeV [28]. Note that the LQCD result for  $f_D$  by ETM [21] quoted in panel (a) is for the isospin-averaged quantity  $f_D$ , whereas the number quoted from FNAL/MILC [19] is for  $f_{D^+}$ . In panel (b) all lattice results are for the isospin-averaged quantity  $f_{D_s}$ . From these, ETM result [21] and the top FNAL/MILC result [19] are  $n_f = 2 + 1 + 1$  calculations and included in the FLAG  $n_f = 2 + 1 + 1$  average [14]. All other LQCD results shown in panel (b) are  $n_f = 2 + 1$  calculations. Comparing these results shows that the effect of adding a charm quark to the sea is very small for  $f_{D_s}$ . Data from Refs. [17–21, 23–26, 29–38]. Figure provided by Hai-Long Ma.

Assuming that the pseudoscalar meson width is negligible, the differential decay rate can be written as

$$\frac{d\Gamma}{dq^2} = \frac{G_F^2}{24\pi^3} |V_{cd(s)}|^2 \frac{(q^2 - m_\ell^2)^2 \sqrt{E_P^2 - M_P^2}}{q^4 M_{D(s)}^2} \times \left[ \left( 1 + \frac{m_\ell^2}{2q^2} \right) M_{D(s)}^2 (E_P^2 - M_P^2) |f_+(q^2)|^2 + \frac{3m_\ell^2}{8q^2} (M_{D(s)}^2 - M_P^2)^2 |f_+(q^2)|^2 \right], \quad (8)$$

where  $E_P$  is the light-pseudoscalar meson energy in the rest frame of the decaying  $D_{(s)}$ ,  $M_P$  and  $M_{D(s)}$  are the meson masses,  $m_\ell$  is the lepton mass, and  $q = (p_{D(s)} - p_P)$  is the momentum of the outgoing lepton pair. The vector and scalar form factors  $f_+(q^2)$  and  $f_0(q^2)$  parameterize the hadronic matrix element of the heavy-to-light quark flavour-changing vector current  $V_\nu = \bar{d}\gamma_\mu c$  (or  $V_\nu = \bar{s}\gamma_\mu c$ ),

$$\langle P | V_\mu | D_{(s)} \rangle = f_+(q^2) \left( (p_{D(s)})_\mu + (p_P)_\mu - \frac{M_{D(s)}^2 - M_P^2}{q^2} q_\mu \right) + f_0(q^2) \frac{M_{D(s)}^2 - M_P^2}{q^2} q_\mu \quad (9)$$

and satisfy the kinematic constraint  $f_+(0) = f_0(0)$ .

The contribution from the scalar form factor to the decay width is proportional to  $m_\ell^2$ , which can usually be neglected. With this assumption, Eq. (8) simplifies to

$$\frac{d\Gamma}{dq^2} = \frac{G_F^2}{24\pi^3} |V_{cs(d)}|^2 p_P^3 |f_+^P(q^2)|^2. \quad (10)$$

From analyses of the dynamics in these semileptonic decays, one can obtain the product of a form factor and a CKM matrix element:  $|V_{cx}| f_+^P(q^2)$ . One can either take  $|V_{cd(s)}|$  from a global fit and extract the form factor by choosing a parameterization (such as a simple pole and  $z$ -expansion), or one can extract  $|V_{cd(s)}|$  by using the form

factor calculated in LQCD. The shapes of the form factors from experiment and LQCD can even be compared without knowledge of the CKM element, which simply appears as a normalisation factor.

The CLEO experiment has made the first high precision measurements of  $D^{0/+} \rightarrow K/\pi e^+ \nu_e$  decay rates based on datasets accumulated at the  $\psi(3770)$  resonance peak with two different methods. The core concept of the double tag method is to take the advantage of the pair production of  $D\bar{D}$  in the  $\psi(3770)$  decays with the four-momentum conservation rule. (Details are introduced in Section IV.) On the tag side, one of the  $D$  mesons is fully reconstructed via a hadronic decay mode, and on the signal side, the semi-leptonic channel is reconstructed by identifying the hadron and  $\ell^+$ . The neutrino is the only missing particle, and thus the missing mass can be used to extract signal events with a low level background. An alternative method does not tag one of the  $D$  mesons and instead uses the entire missing energy and momentum in an event to access to the four momentum of the missing neutrino. The CLEO experiment once used this method, but the large backgrounds make it much less popular than the the double tag method.

In the past ten years, BESIII, with a triple amount of  $\psi(3770)$  data, reported measurements of these absolute decay rates and accordingly the products of the hadronic form factors at  $q^2 = 0$  and the magnitude of the CKM matrix elements with significantly improved precision. BESIII studied the semi-leptonic  $D_{(s)}^{0(+)}$  decays into  $P$ ,  $V$ ,  $S$ , and  $A$ , where  $P$  denotes pseudoscalar mesons of  $K$  [40–47],  $\pi$  [40, 41, 48],  $\eta$  [49–53],  $\eta'$  [49, 51–53];  $V$  denotes vector mesons of  $K^*$  [54, 55],  $\rho$  [56, 57],  $\omega$  [58, 59], and  $\phi$  [53, 58];  $S$  denotes scalar mesons of  $f_0$  [56, 60] and  $a_0$  [61, 62]; and  $A$  denotes axial vector mesons of  $K_1$  [63, 64] and  $b_1$  [65]. These measurements were carried out by using 2.93, 0.48, and 6.32  $\text{fb}^{-1}$  of data taken at  $\sqrt{s} = 3.773, 4.009, \text{ and } 4.178\text{--}4.226$  GeV. From studies of the differential decay rates (see Eq.( 10)) and the values of  $|V_{cd}|$  and  $|V_{cs}|$  from the SM-constrained fit [1], one can extract the transition form factors. The best precision of the  $c \rightarrow s$  and  $c \rightarrow d$  semi-leptonic  $D^{0(+)}$  decay form factors are from the studies of  $D^{0(+)} \rightarrow \bar{K}\ell^+\nu_\ell$  and  $D^{0(+)} \rightarrow \pi\ell^+\nu_\ell$  (shown in Fig. 4).

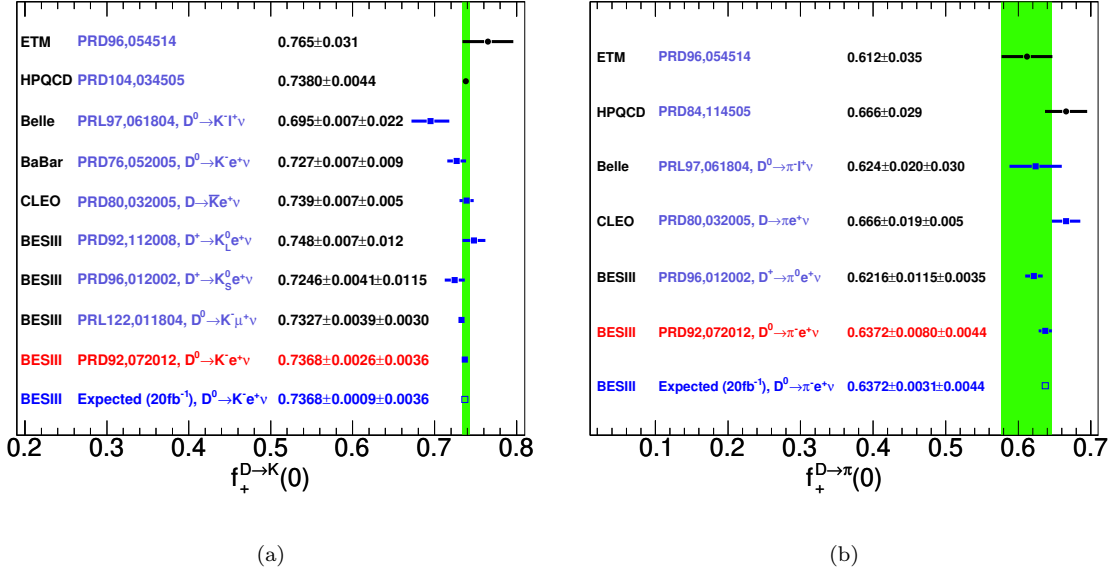


FIG. 4. Comparison of the results for (a)  $f_+^K(0)$  and (b)  $f_+^\pi(0)$  measured by the Belle, BaBar, CLEO-c and BESIII experiments. The green bands present the lattice quantum chromodynamics (LQCD) uncertainties. Values marked in black circle denote LQCD calculations, values marked in blue square denotes experimental results, and the value marked in open square denotes the expected precision from BESIII with 20  $\text{fb}^{-1}$  data set at 3.773 GeV [28]. Note that the lattice calculation of  $f_+^{D \rightarrow \pi}$  by HPQCD Collaboration [66] was done using  $n_f = 2 + 1$  flavors of sea quarks, whereas HPQCD Collaboration's calculation of  $f_+^{D \rightarrow K}$  [67] and ETM Collaboration's calculation [68] include charm quarks in the sea. These latter two calculations are included in the FLAG  $n_f = 2 + 1 + 1$  average. Data from Refs. [40–42, 45, 66, 67, 69–72]. Figure provided by Hai-Long Ma.

LQCD computations of  $f_+$  allow for comparisons to experiment to ascertain whether the SM provides the correct prediction for the  $q^2$ -dependence of  $d\Gamma(D_{(s)} \rightarrow P\ell\nu_\ell)/dq^2$  and, subsequently, to determine the CKM matrix elements  $|V_{cd}|$  and  $|V_{cs}|$ . As for the decay constants, we use the FLAG averages [14] of the lattice calculations with  $n_f = 2 + 1 + 1$  sea quarks. Results included in the average come from the ETM collaboration [69] and the HPQCD Collaboration [67]. Knowing the value of the form factor  $f_+$  at  $q^2 = 0$  is enough to determine the CKM element, and historically those

values are usually quoted. The result for  $f_+(0)$  for  $D \rightarrow \bar{K}\ell\nu_\ell$  is very precise with a 0.6% uncertainty, whereas  $f_+(0)$  for  $D \rightarrow \pi\ell\nu_\ell$  has an uncertainty of almost 6%. The lattice results are shown along experimental results in Fig. 4 and Table II.

The most commonly used parameterization of the form factors is the  $z$ -expansion:

$$f(q^2) = \frac{1}{B(q^2)\phi(q^2, t_0)} \sum_{n=0}^N a_n z^n, \quad z(q^2, t_0) = \frac{\sqrt{t_+ - q^2} - \sqrt{t_+ - t_0}}{\sqrt{t_+ - q^2} + \sqrt{t_+ - t_0}}, \quad (11)$$

which exploits the positivity and analyticity properties of two-point functions of vector currents. This is a conformal transformation that maps the  $q^2$  plane cut for  $q^2 \geq t_+$  onto the disk  $|z(q^2, t_0)| < 1$  in the  $z$  complex plane. Here  $t_+ = (M_{D^{(s)}} + M_P)^2$  (the meson  $P$  being  $\pi$  or  $K$ ), and the real parameter  $t_0$  can be chosen freely as long as  $t_0 < t_+$ . A common choice is  $t_0 = t_+(1 - (1 - t_-/t_+)^{1/2})$ , which minimises the maximum value of  $z$  over the  $q^2$  range of the decay.  $B(q^2)$  is the Blaschke factor, which contains poles and cuts below  $t_+$ . Common choices are  $B(q^2) = 1 - q^2/M_{\text{pole}}^2$ , where  $M_{\text{pole}}$  is the pole mass, or  $B(q^2) = z(q^2, M_{\text{pole}}^2)$ . The so-called outer function  $\phi(q^2, t_0)$  can have a more complicated  $q^2$  dependence, or it can be chosen to be  $\phi(q^2, t_0) = 1$ .

If one uses the same  $z$ -expansion to fit lattice form factors and different experimental data sets, or uses a 'refitting' procedure as in [67], one can compare the shapes of the form factors extracted from each data set by looking at ratios of the coefficients  $a_n$  of the  $z$ -expansion. (See [67] Eq. B2 for the outer function  $\phi(q^2, t_0)$  used there.) Since the CKM element cancels in the ratio, the comparison is direct. This is shown in Fig. 5 (which is from [67]), comparing form factors extracted from CLEO [72], BaBar [71], BESIII [40] as well as the HFLAV experimental average [81] and the LQCD determination by HPQCD [67]. The agreement is seen to be good, and possible tensions in the shape of the form factor between theory and experiment or between different experiments would be apparent in a comparison like this one.

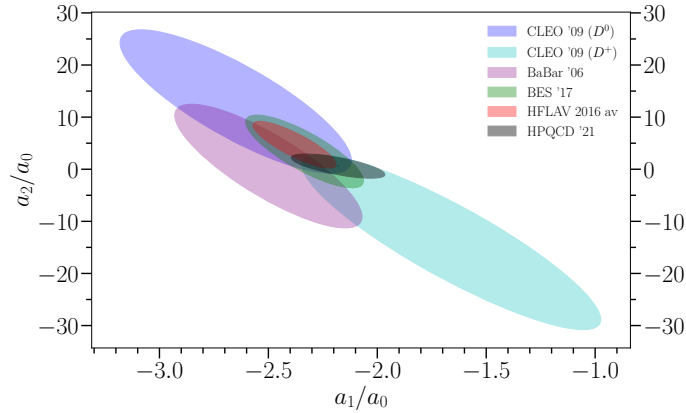


FIG. 5. Comparison of the shape of the vector form factor for  $D \rightarrow \bar{K}\ell\nu_\ell$  expressed in terms of ratios of the  $z$ -expansion coefficients. Ellipses give the 68% confidence limits ( $\Delta\chi^2 = 2.3$ ). Experimental results are from [40, 71, 72, 81]. CLEO results are for  $D^0 \rightarrow K^- e^+ \nu_e$  (dark blue) and  $D^+ \rightarrow \bar{K}^0 e^+ \nu_e$  (light blue); all other experimental data is for  $D^0 \rightarrow K^- e^+ \nu_e$ . The HFLAV experimental average [81] is given as the red ellipse. The black ellipse gives the LQCD result by the HPQCD Collaboration [67]. Good agreement is seen between the experimental results and the LQCD result. Figure from [67].

The FLAG review [14] also provides  $z$ -expansion parameterizations of the form factors for the  $D \rightarrow \bar{K}\ell\nu_\ell$  decay. They adopt the standard implementation of the Bourrely-Caprini-Lellouch (BCL) parameterization [82], which is widely used by experimental and LQCD collaborations:

$$f_+(q^2) = \frac{1}{1 - q^2/(M_{\text{pole}}^V)^2} \sum_{n=0}^{N-1} a_n^+ \left[ z^n - (-1)^{n-N} \frac{n}{N} z^N \right],$$

$$f_0(q^2) = \frac{1}{1 - q^2/(M_{\text{pole}}^S)^2} \sum_{n=0}^{N-1} a_n^0 z^n, \quad (12)$$

TABLE II. Measurements of  $D^0/D^+$ ,  $D_s^+$  and  $\Lambda_c^+$  semi-leptonic decays with near-threshold data at BESIII and comparisons between experimental results and theoretical expectations or SM-global fit result. (Here “-” indicates not available.) For theory predictions of the form factors at  $q^2 = 0$ , we take the Flavour Lattice Averaging Group (FLAG) averages [14] of calculations with  $n_f = 2 + 1 + 1$  sea quarks. The original calculations included in the average are cited next to the result. Note that these predictions, which are marked with an asterisk in the table, are for the isospin-averaged quantities. The calculation of  $\Lambda_c$  form factors [73] used  $n_f = 2 + 1$  sea quark flavors. There are currently several ongoing lattice calculations to extract the  $D_s \rightarrow K$  form factors [74, 75]. In earlier lattice calculations the  $D \rightarrow \pi$  and  $D_s \rightarrow K$  form factors have been found to be the same within few % [76, 77]. The shape of the form factor is very insensitive to the spectator quark (here  $u$  or  $s$ ).

Observable	Measurement	Prediction/Fit
$\mathcal{B}(D^0 \rightarrow K^- e^+ \nu_e)$	$(3.505 \pm 0.014_{\text{stat}} \pm 0.033_{\text{syst}})\%$ [40]	-
$ V_{cs} f_+^{D \rightarrow K}(0)$	$0.7172 \pm 0.0025_{\text{stat}} \pm 0.0035_{\text{syst}}$	-
$f_+^{D \rightarrow K}(0)$	$0.7368 \pm 0.0026_{\text{stat}} \pm 0.0036_{\text{syst}}$	$0.7385 \pm 0.0044^*$ [67, 69]
$\mathcal{B}(D^0 \rightarrow K^- \mu^+ \nu_\mu)$	$(3.413 \pm 0.019_{\text{stat}} \pm 0.035_{\text{syst}})\%$ [45]	-
$ V_{cs} f_+^{D \rightarrow K}(0)$	$0.7133 \pm 0.0038_{\text{stat}} \pm 0.0030_{\text{syst}}$	-
$f_+^{D \rightarrow K}(0)$	$0.7327 \pm 0.0039_{\text{stat}} \pm 0.0030_{\text{syst}}$	$0.7385 \pm 0.0044^*$ [67, 69]
$\mathcal{B}(D^0 \rightarrow K^- \mu^+ \nu_\mu)/\mathcal{B}(D^0 \rightarrow K^- e^+ \nu_e)$	$0.974 \pm 0.007_{\text{stat}} \pm 0.012_{\text{syst}}$ [45]	$0.9779 \pm 0.0050$ [67]
$\mathcal{B}(D^0 \rightarrow \pi^- e^+ \nu_e)$	$(0.295 \pm 0.004_{\text{stat}} \pm 0.003_{\text{syst}})\%$ [40]	-
$ V_{cd} f_+^{D \rightarrow \pi}(0)$	$0.1435 \pm 0.0018_{\text{stat}} \pm 0.0009_{\text{syst}}$	-
$f_+^{D \rightarrow \pi}(0)$	$0.6372 \pm 0.0080_{\text{stat}} \pm 0.0044_{\text{syst}}$	$0.612 \pm 0.035^*$ [69]
$\mathcal{B}(D^+ \rightarrow \bar{K}^0 e^+ \nu_e)$	$(8.60 \pm 0.06_{\text{stat}} \pm 0.15_{\text{syst}})\%$ [41]	-
$f_+^{D \rightarrow K}(0)$	$0.725 \pm 0.004_{\text{stat}} \pm 0.012_{\text{syst}}$	$0.7385 \pm 0.0044^*$ [67, 69]
$\mathcal{B}(D^+ \rightarrow \pi^0 e^+ \nu_e)$	$(0.363 \pm 0.008_{\text{stat}} \pm 0.005_{\text{syst}})\%$ [41]	-
$f_+^{D \rightarrow \pi}(0)$	$0.622 \pm 0.012_{\text{stat}} \pm 0.003_{\text{syst}}$	$0.612 \pm 0.035^*$ [69]
$f_+^{D \rightarrow \pi}(0)/f_+^{D \rightarrow K}(0)$	$0.865 \pm 0.013$ [41]	$0.84 \pm 0.04$ [78]
$\mathcal{B}(D^+ \rightarrow \eta e^+ \nu_e)$	$(10.74 \pm 0.81_{\text{stat}} \pm 0.51_{\text{syst}}) \times 10^{-4}$ [49]	-
$ V_{cd} f_+^{D \rightarrow \eta}(0)$	$0.0079 \pm 0.0006_{\text{stat}} \pm 0.0002_{\text{syst}}$	-
$\mathcal{B}(D^+ \rightarrow \eta \mu^+ \nu_\mu)$	$(10.4 \pm 1.0_{\text{stat}} \pm 0.5_{\text{syst}}) \times 10^{-4}$ [50]	-
$ V_{cd} f_+^{D \rightarrow \eta}(0)$	$0.0087 \pm 0.0008_{\text{stat}} \pm 0.0002_{\text{syst}}$	-
$f_+^{D \rightarrow \eta}(0)$	$0.39 \pm 0.04_{\text{stat}} \pm 0.01_{\text{syst}}$	-
$\mathcal{B}(D^+ \rightarrow \eta \mu^+ \nu_\mu)/\mathcal{B}(D^+ \rightarrow \eta e^+ \nu_e)$	$0.91 \pm 0.13$	-
$\mathcal{B}(D_s^+ \rightarrow \eta e^+ \nu_e)$	$(2.323 \pm 0.063_{\text{stat}} \pm 0.063_{\text{syst}})\%$ [51]	-
$ V_{cs} f_+^{D_s \rightarrow \eta}(0)$	$0.4455 \pm 0.0053_{\text{stat}} \pm 0.0044_{\text{syst}}$	-
$f_+^{D_s \rightarrow \eta}(0)$	$0.4576 \pm 0.0054_{\text{stat}} \pm 0.0045_{\text{syst}}$	-
$\mathcal{B}(D_s^+ \rightarrow \eta' e^+ \nu_e)$	$(2.323 \pm 0.063_{\text{stat}} \pm 0.063_{\text{syst}})\%$ [51]	-
$ V_{cs} f_+^{D_s \rightarrow \eta'}(0)$	$0.477 \pm 0.049_{\text{stat}} \pm 0.011_{\text{syst}}$	-
$f_+^{D_s \rightarrow \eta'}(0)$	$0.490 \pm 0.050_{\text{stat}} \pm 0.011_{\text{syst}}$	-
$\mathcal{B}(D_s^+ \rightarrow K^0 e^+ \nu_e)$	$(3.25 \pm 0.38_{\text{stat}} \pm 0.16_{\text{syst}})\%$ [47]	-
$ V_{cd} f_+^{D_s \rightarrow K}(0)$	$0.162 \pm 0.019_{\text{stat}} \pm 0.003_{\text{syst}}$	-
$f_+^{D_s \rightarrow K}(0)$	$0.720 \pm 0.084_{\text{stat}} \pm 0.013_{\text{syst}}$	$f^{D_s \rightarrow K}(0) \approx f^{D \rightarrow \pi}(0)$ within 5% [76, 77]
$\mathcal{B}(\Lambda_c^+ \rightarrow \Lambda e^+ \nu_e)$	$(3.56 \pm 0.11_{\text{stat}} \pm 0.07_{\text{syst}})\%$ [12]	$3.55 \pm 1.04\%$ [79]
$\alpha_1^{g\perp}$	$1.43 \pm 2.09_{\text{stat}} \pm 0.16_{\text{syst}}$	-
$\alpha_1^{f\perp}$	$-8.15 \pm 1.58_{\text{stat}} \pm 0.05_{\text{syst}}$	-
$r_{f\perp}$	$1.75 \pm 0.32_{\text{stat}} \pm 0.01_{\text{syst}}$	-
$r_{g\perp}$	$3.62 \pm 0.65_{\text{stat}} \pm 0.02_{\text{syst}}$	-
$r_{g\perp}$	$1.13 \pm 0.13_{\text{stat}} \pm 0.01_{\text{syst}}$	-
$\mathcal{B}(\Lambda_c^+ \rightarrow \Lambda \mu^+ \nu_\mu)$	$(3.49 \pm 0.46_{\text{stat}} \pm 0.27_{\text{syst}})\%$ [13]	-
$\mathcal{B}(\Lambda_c^+ \rightarrow \Lambda \mu^+ \nu_\mu)/\mathcal{B}(\Lambda_c^+ \rightarrow \Lambda e^+ \nu_e)$	$0.96 \pm 0.16_{\text{stat}} \pm 0.04_{\text{syst}}$	$\approx 1.0$ [80]
$\Gamma(\Lambda_c \rightarrow \Lambda e^+ \nu_e)/ V_{cs} ^2$	-	$0.2007 \pm 0.0071_{\text{stat}} \pm 0.0074_{\text{syst}} \text{ ps}^{-1}$ [73]
$\Gamma(\Lambda_c \rightarrow \Lambda \mu^+ \nu_\mu)/ V_{cs} ^2$	-	$0.1945 \pm 0.0069_{\text{stat}} \pm 0.0072_{\text{syst}} \text{ ps}^{-1}$ [73]

where  $M_{\text{pole}}^V$  is the vector pole mass ( $D_s^*$  mass in the case of  $D \rightarrow \bar{K} \ell \nu_\ell$  decay), and  $M_{\text{pole}}^S$  is the scalar pole mass ( $D_{s0}$  mass for charm-to-strange decay). This is illustrated in Fig. 6, which shows FLAG's fit to lattice data only (normalizing the fit result for the plot with their choice of  $|V_{cs}|$ ) and also their combined fit to both lattice and experimental data (in which case  $|V_{cs}|$  can be extracted from the fit).

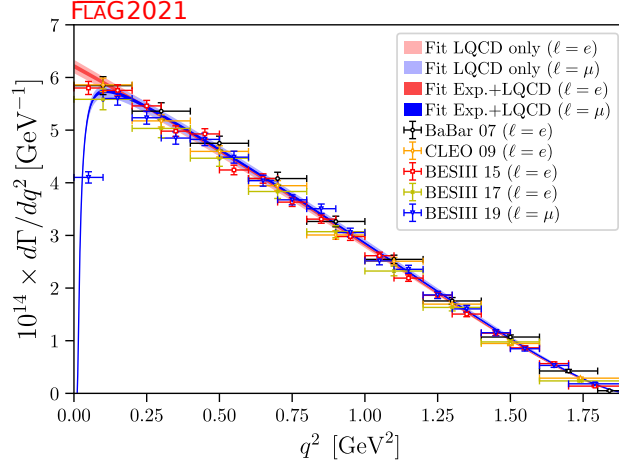


FIG. 6. The  $D \rightarrow \bar{K} \ell \nu_\ell$  differential decay rates from the FLAG 2021 review [14]. This illustrates the FLAG fit to LQCD data and to LQCD+experimental data (see section 7 of the review for further details on the fits).

The FLAG  $n_f = 2 + 1 + 1$  averages [14] for the CKM elements from these fits are [67, 69, 83]

$$|V_{cd}| = 0.2341 \pm 74 \quad (13)$$

$$|V_{cs}| = 0.9714 \pm 69 \quad (14)$$

The experimental data sets included in the fit for  $|V_{cd}|$  are  $D^0 \rightarrow \pi^- e^+ \nu_e$  from BaBar [84],  $D^0 \rightarrow \pi^- e^+ \nu_e$  and  $D^+ \rightarrow \pi^0 e^+ \nu_e$  from CLEO-c [72],  $D^0 \rightarrow \pi^- e^+ \nu_e$  and  $D^+ \rightarrow \pi^0 e^+ \nu_e$  from and BESIII [40, 41]. In the extraction of  $|V_{cs}|$  the experimental data consist of  $D^0 \rightarrow K^- e^+ \nu_e$  from BaBar [71], CLEO-c [72] and BESIII [40];  $D^+ \rightarrow \bar{K}^0 e^+ \nu_e$  from CLEO-c [72] and BESIII [41]; and  $D^0 \rightarrow K^- \mu^+ \nu_\mu$  from BESIII [45]. Given the form factor  $f_+(q^2)$  from LQCD, one can integrate (numerically) Eq. (10) over  $q^2$  bins and extract the CKM element bin-by-bin basis by taking the ratio with the experimental value for that bin. Any tensions between the shapes of the form factors from different data sets would again be distinct.

To study the  $c \rightarrow d$  transition, one can also look at the  $D_s^+ \rightarrow K^0 e^+ \nu_e$  decay, in addition to  $D^0 \rightarrow \pi^- e^+ \nu_e$  and  $D^+ \rightarrow \pi^0 e^+ \nu_e$ . The difference between these decays is the spectator quark, which is here either  $s$  or  $u$  quark. There are currently several ongoing lattice calculations to extract the  $D_s \rightarrow K \ell \nu$  form factors [74, 75]. In earlier lattice calculations the  $D \rightarrow \pi \ell \nu$  and  $D_s \rightarrow K \ell \nu$  form factors have been found to be the same within few % in the whole  $q^2$  range allowed by kinematics [76, 77]. The shape of the form factor is very insensitive to the spectator quark.

In addition to  $D_{(s)}$  meson semileptonic decays to a single pseudoscalar meson (plus the lepton and its neutrino), BESIII has reported the partial wave analyses of  $D^{0(+)} \rightarrow \pi^{0(+)} \pi^- e^+ \nu_e$  [56] and  $D^+ \rightarrow K^- \pi^+ e^+ \nu_e$  [54, 55], and measures the parameters of the corresponding form factors. BESIII also has observed the  $D^{0(+)}$  to axial-vector particle semileptonic decays,  $D^{0(+)} \rightarrow K_1(1270)^-(0) e^+ \nu_e$  [63, 64], and  $D^{0(+)}$  to scalar particle semileptonic decays,  $D^{0(+)} \rightarrow a_0(980)^-(0) e^+ \nu_e$  [61] for the first time. These studies on the intermediate resonances in hadronic final states, e.g.,  $K_1(1270)$ ,  $K^*(980)$ ,  $f_0(980)$ , and  $a_0(980)$ , in the semileptonic  $D_{(s)}^{0(+)}$  decays provide a clean environment to explore meson spectroscopy, as no other particles interfere. This is a major advantage in comparison to hadronic spectroscopy studies in charmonium decay or hadronic  $D_{(s)}$  decays.

The  $D_s^+$  to vector meson semi-leptonic decay  $D_s^+ \rightarrow \phi \ell^+ \nu_\ell$  offers another independent approach to  $|V_{cs}|$ . The first experimental measurement is reported by Babar [85]. On the theory side, there is a LQCD calculation of the decay [86], which is more complicated as there are more form factors involved. This calculation was done using  $n_f = 2 + 1$  sea quarks. In [86] the authors also extracted the  $q^2$  and angular distributions for the differential rate and found good agreement with those from the BaBar experiment. From the total branching fraction they obtain  $|V_{cs}| = 1.017(63)$ , in good agreement with that from  $D \rightarrow \bar{K} \ell \nu_\ell$  semileptonic decay.

A similar approach can be applied to the charmed baryon semi-leptonic decays. Among the  $\Lambda_c^+$  semileptonic decays,  $\Lambda_c^+ \rightarrow \Lambda \ell^+ \nu_\ell$  is the only dominant one. BESIII, using the similar tag technique employed in the  $D\bar{D}$  threshold production, measures the absolute branching fraction of  $\Lambda_c^+ \rightarrow \Lambda e^+ \nu_e$  and the  $\Lambda_c^+ \rightarrow \Lambda$  form factors for the first time based on  $4.5 \text{ fb}^{-1}$   $\Lambda_c^+ \bar{\Lambda}_c^-$  dataset collected at 4.600-4.699 GeV [12, 87]. The  $\bar{\Lambda}_c^-$  is reconstructed via its hadronic decay modes and the missing neutrino on the signal side is inferred by the kinematic variable  $U_{\text{miss}} = E_{\text{miss}} - c|\vec{p}_{\text{miss}}|$ , where  $E_{\text{miss}}$  and  $\vec{p}_{\text{miss}}$  are the missing energy and missing momentum, respectively. The  $U_{\text{miss}}$  distribution is presented in Fig. 7. The measured branching fractions of  $\Lambda_c^+ \rightarrow \Lambda e^+ \nu_e$  and  $\Lambda_c^+ \rightarrow \Lambda \mu^+ \nu_\mu$ , and their ratio are given in Table II. Four form factors  $f_{\perp,+}(q^2)$  and  $g_{\perp,+}(q^2)$  are necessary to parameterize the dynamics, defined following a  $z$ -expansion:

$$f(q^2) = \frac{a_0^f}{1 - q^2/m_{\text{pole}}^f} \left[ 1 + \alpha_1^f \times z(q^2) \right], \quad (15)$$

where  $m_{\text{pole}}^f$  is the pole mass;  $a_0^f, \alpha_1^f$  are free parameters;  $z(q^2) = \frac{(\sqrt{t_+ - q^2} - \sqrt{t_+ - t_0})}{(\sqrt{t_+ - q^2} + \sqrt{t_+ - t_0})}$  with  $t_0 = q_{\text{max}}^2 = (m_{\Lambda_c} - m_\Lambda)^2$ ,  $t_+ = (m_D + m_K)^2$ ,  $m_D = 1.870 \text{ GeV}/c^2$  and  $m_K = 0.494 \text{ GeV}/c^2$ . The pole masses  $m_{\text{pole}}^{f+,f\perp}$  and  $m_{\text{pole}}^{g+,g\perp}$  are fixed to 2.112 and 2.460  $\text{GeV}/c^2$ , respectively [73]. Setting  $\alpha_1^{\perp+} \equiv \alpha_1^{g+}$  and  $\alpha_1^{f\perp+} \equiv \alpha_1^{g\perp+}$ , BESIII measures  $\alpha_1^{\perp+}, \alpha_1^{f\perp+}$ ,  $r_{f_+} = a_0^{f_+}/a_0^{g_+}, r_{f_\perp} = a_0^{f_\perp}/a_0^{g_\perp}$ , and  $r_{g_+} = a_0^{g_+}/a_0^{g_\perp}$ , given in Table II. In addition, BESIII reports the observation of  $\Lambda_c^+ \rightarrow pK^- e^+ \nu_e$  and evidence for  $\Lambda_c^+ \rightarrow \Lambda^*(1520)e^+ \nu_e$  [88].

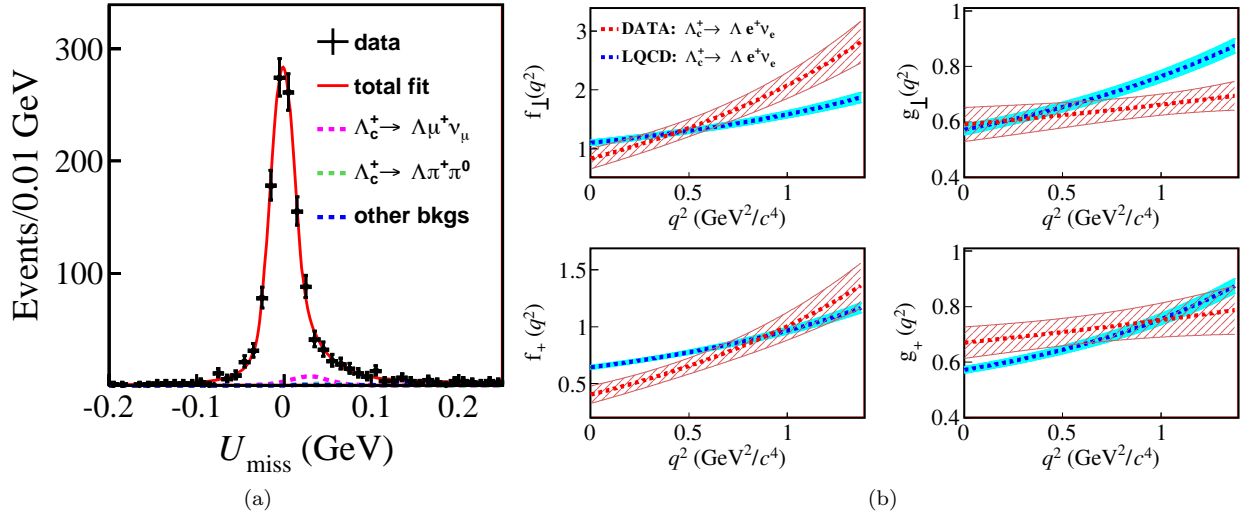


FIG. 7. (a) Fit to the  $U_{\text{miss}}$  distribution within the  $\Lambda$  signal region [12]. The points with error bars are data, the solid curves show the total fits, and the dashed curves are the background shapes. (b) Comparison of the form factors with a lattice quantum chromodynamics (LQCD) calculation [73]. The bands show the total uncertainties. Figure from Ref. [12].

There exists one LQCD calculation of the  $\Lambda_c^+ \rightarrow \Lambda \ell^+ \nu_\ell$  form factors and decay rates by Meinel [73]. The main results of the paper are the LQCD predictions for the decay rates:  $\Gamma(\Lambda_c^+ \rightarrow \Lambda e^+ \nu_e)/|V_{cs}|^2 = 0.2007 \pm 71 \pm 74 \text{ ps}^{-1}$  and  $\Gamma(\Lambda_c^+ \rightarrow \Lambda \mu^+ \nu_\mu)/|V_{cs}|^2 = 0.1945 \pm 69 \pm 72 \text{ ps}^{-1}$ , where the first uncertainties are statistical and the second ones are systematic uncertainties. Combining their results with BESIII measurements of the branching fractions [13, 87] and using  $\tau_{\Lambda_c} = 0.200 \pm 6 \text{ ps}$  they extract the CKM element

$$|V_{cs}| = \begin{cases} 0.951 \pm 24_{\text{LQCD}} \pm 14_{\tau_{\Lambda_c}} \pm 56_{\mathcal{B}}, & \ell = e, \\ 0.947 \pm 24_{\text{LQCD}} \pm 14_{\tau_{\Lambda_c}} \pm 72_{\mathcal{B}}, & \ell = \mu, \\ 0.949 \pm 24_{\text{LQCD}} \pm 14_{\tau_{\Lambda_c}} \pm 49_{\mathcal{B}}, & \ell = e, \mu, \end{cases} \quad (16)$$

where the last line is the correlated average over  $\ell = e, \mu$ . The LQCD form factors and the new BESIII results [12] are compared in Fig. 7 (b). Some tensions can be observed between the shapes of the form factors, but smaller uncertainties are needed to draw any conclusions.

In addition, there is a LQCD determination of the  $\Lambda_c^+ \rightarrow N$  (where  $N$  is a proton or a neutron) vector, axial vector, and tensor form factors [89]. The results provide SM predictions for the  $\Lambda_c^+ \rightarrow n e^+ \nu_e$  and  $\Lambda_c^+ \rightarrow n \mu^+ \nu_\mu$  decay rates

with an uncertainty of 6.4%. These modes can be only studied with double-tag method which is unique at BESIII, and they are in the list of the BESIII charmed baryon project. The form factors can also be applied to study the differential branching fraction and angular distribution of the rare charm decay  $\Lambda_c^+ \rightarrow p\mu^+\mu^-$ , using perturbative results for the effective Wilson coefficients in the SM.

Besides  $\Lambda_c^+$ , there are also studies for semileptonic decays of charmed baryon  $\Xi_c^{+,0}$  and  $\Omega_c^0$ . The  $\Xi_c^{+,0} \rightarrow \Xi^{0,-}$ , like  $\Lambda_c^+ \rightarrow \Lambda$ , are  $1/2^+ \rightarrow 1/2^+$  transitions, which allows a relatively simple theoretical calculation of form factors and hadronic structures under nonperturbative QCD. The authors of [90] recently performed the first LQCD calculation of the  $\Xi_c \rightarrow \Xi\ell\nu_\ell$  form factors. This calculation uses two lattice ensembles with different lattice spacings and  $n_f = 2 + 1$  sea quark flavours. The pion masses on both ensembles are unphysical and nearly identical, 290 MeV and 300 MeV. The results are extrapolated to the continuum limit, but are not extrapolated to the physical pion mass. Therefore the error budget is not complete, as systematic uncertainty for the effect of the missing chiral extrapolation is not estimated. However, this is an important first step and shows that LQCD calculations of  $\Xi_c$  form factors are now feasible.

For the  $\Omega_c^0$  weak decays, most decay channels involve non-factorizable effects. Nonetheless,  $\Omega_c^0 \rightarrow \Omega^- M^+$  with  $M = (\pi, \rho)$  and  $\Omega_c^0 \rightarrow \Omega^- \ell^+ \nu_\ell$  with  $\ell = (e, \mu)$  proceed through the  $\Omega_c^0 \rightarrow \Omega^-$ , which is a  $1/2^+ \rightarrow 3/2^+$  transition, along with the external  $W$ -boson emitted to connect  $M^+$  or  $\ell^+ \nu_\ell$ . There exist eight form factors for the  $\Omega_c^0 \rightarrow \Omega^-$  transition, two more than that in  $1/2^+ \rightarrow 1/2^+$  transitions, which play the key role in calculating  $\mathcal{B}(\Omega_c^0 \rightarrow \Omega^- M^+)$  and  $\mathcal{B}(\Omega_c^0 \rightarrow \Omega^- e^+ \nu_e)$  [91–95]. Belle, CLEO II, and ALICE have performed the most precise branching fraction measurement of  $\Xi_c^{+,0} \rightarrow \Xi^{0,-} \ell^+ \nu_\ell$  [96–98], and the branching ratios  $\mathcal{B}(\Omega_c^0 \rightarrow \Omega^- e^+ \nu_e)/\mathcal{B}(\Omega_c^0 \rightarrow \Omega^- \pi^+)$  [99, 100] while the experimental results are not well consistent with the theoretical predictions. The relevant studies are summarized in Table III.

### C. Discussion: $|V_{cd}|$ and $|V_{cs}|$ determinations

The LQCD theory has made an admirable achievement in the past decade, improving the uncertainties of calculated decay constants from the level of 1-2% to 0.33% ( $f_D$ ) and 0.2% ( $f_{D_s}$ ) [14]. The experiments have not quite been able to keep up the pace: the current PDG world average values of  $|V_{cd}|$  and  $|V_{cs}|$  struggle with uncertainties of 2.5% and 1.5%, respectively, which are dominated by the BESIII leptonic-decay measurements. In these measurements, the systematic uncertainty on  $|V_{cd}|$  is smaller than its statistical uncertainty, while the statistical and systematic uncertainties of  $|V_{cs}|$  are comparable, as shown in Fig. 8.

In addition, the measurements of the charmed-meson semi-leptonic decays  $D^{0(+)} \rightarrow \bar{K}\ell\nu_\ell$  and  $D^{0(+)} \rightarrow \pi\ell\nu_\ell$  with form factors from LQCD calculations as the key inputs [14] offer a completely different way of extracting  $|V_{cs}|$  and  $|V_{cd}|$ . The experimental data and the latest  $n_f = 2 + 1 + 1$  LQCD results on  $D \rightarrow \bar{K}\ell\nu_\ell$  decay are so precise, that  $|V_{cs}|$  can be determined with  $\leq 1\%$  accuracy. In [67] the authors tested three different ways of determining  $|V_{cd}|$  from their LQCD form factors and experimental data: 1) using the full kinematic  $q^2$  range and differential branching fractions  $d\Gamma/dq^2$ ; 2) using their determination of the value of the form factor at  $q^2 = 0$ ,  $f_+(0)$ , and experimental determinations of  $|V_{cs}|f_+(0)$ ; 3) Using the integrated, total branching fraction  $\mathcal{B}$ , integrating the LQCD form factor over the whole  $q^2$  range. All three methods gave results that are within  $0.6\sigma$ , and with similar precision. However, the lattice results for  $D \rightarrow \pi\ell\nu_\ell$  have much larger uncertainties. In this review we have opted to use the  $N_f = 2 + 1 + 1$  FLAG results [14] for both  $D \rightarrow \bar{K}\ell\nu_\ell$  and  $D \rightarrow \pi\ell\nu_\ell$  decays for consistency, even though the  $n_f = 2 + 1$  lattice results for the latter decay have 4.4% uncertainty compared to 5.7% for the  $n_f = 2 + 1 + 1$  results. The situation should improve in the next year or so, as two lattice collaborations are working on extracting the  $D \rightarrow \pi\ell\nu_\ell$  form factors with better precision [74, 75]. The anticipated uncertainties should allow the extraction of  $V_{cd}$  from semileptonic decays to precision of  $\sim 1\%$ .

Let us now collect and compare the results from leptonic and semileptonic decays for the CKM elements:

$$\begin{aligned} |V_{cd}|^{\text{lept}} &= 0.2179 \pm 57, & |V_{cs}|^{\text{lept}} &= 0.983 \pm 18 \\ |V_{cd}|^{\text{SL}} &= 0.2341 \pm 74, & |V_{cs}|^{\text{SL}} &= 0.9714 \pm 69 \\ |V_{cd}|^{\text{SM}} &= 0.22486 \pm 67, & |V_{cs}|^{\text{SM}} &= 0.97349 \pm 16. \end{aligned} \tag{17}$$

The first two rows, the leptonic and semileptonic (SL) determinations, are the  $n_f = 2 + 1 + 1$  results from the FLAG



TABLE III. Measurements of  $\Xi_c$ ,  $\Omega_c$  semi-leptonic decays and comparisons between experimental results and theoretical expectations. The theoretical works of LQCD, LCSR, SU(3), LFQM, RQM, and QCDSR are compared. Abbreviations: LCSR, light-cone QCD sum rules; LFQM, light-front quark model; LQCD, lattice QCD. (Here “-” indicates not available.)

Observable/Measurement	experiment	Prediction/Fit
$\mathcal{B}(\Xi_c^0 \rightarrow \Xi^- e^+ \nu_e)$ = $(1.31 \pm 0.04_{\text{stat}} \pm 0.07_{\text{syst}} \pm 0.38_{\Xi_c^0 \rightarrow \Xi^- \pi^+})\%$ [96]	Belle	$2.38 \pm 0.30_{\text{stat}} \pm 0.32_{\text{syst}}\%$ [90] (LQCD)
		$4.10 \pm 0.46\%$ [101] (SU(3))
		$(3.0 \pm 0.3, 2.4 \pm 0.3, 2.7 \pm 0.2)\%$ [102] (SU(3))
		$3.4 \pm 1.7\%$ [103] (QCDSR)
		$3.49 \pm 0.95\%$ [79] (LFQM)
		$1.72 \pm 0.35\%$ [104] (LFQM)
		$7.26 \pm 2.54\%$ [105] (LCSR)
		$1.85 \pm 0.56\%$ [106] (LCSR)
		$2.81^{+0.17}_{-0.15}\%$ [107] (LCSR)
		$1.35\%$ [108] (LFQM)
		$2.38\%$ [109] (RQM)
$\mathcal{B}(\Xi_c^0 \rightarrow \Xi^- \mu^+ \nu_\mu)$ = $(1.27 \pm 0.06_{\text{stat}} \pm 0.10_{\text{syst}} \pm 0.37_{\Xi_c^0 \rightarrow \Xi^- \pi^+})\%$ [96]	Belle	$2.29 \pm 0.29_{\text{stat}} \pm 0.31_{\text{syst}}\%$ [90] (LQCD)
		$3.98 \pm 0.57\%$ [101] (SU(3))
		$3.34 \pm 0.94\%$ [79] (LFQM)
		$7.15 \pm 2.50\%$ [105] (LCSR)
		$1.79 \pm 0.54\%$ [106] (LCSR)
		$2.72^{+0.17}_{-0.15}\%$ [107] (LCSR)
		$2.31\%$ [109] (RQM)
$\mathcal{B}(\Xi_c^0 \rightarrow \Xi^- e^+ \nu_e)/\mathcal{B}(\Xi_c^0 \rightarrow \Xi^- \mu^+ \nu_\mu)$ = $1.03 \pm 0.05_{\text{stat}} \pm 0.07_{\text{syst}}$ [96]	Belle	$\approx 1.0$ [80]
$\mathcal{B}(\Xi_c^0 \rightarrow \Xi^- e^+ \nu_e)/\mathcal{B}(\Xi_c^0 \rightarrow \Xi^- \pi^+)$ = $1.38 \pm 0.14_{\text{stat}} \pm 0.22_{\text{syst}}$ [97]	ALICE	-
$\mathcal{B}(\Xi_c^+ \rightarrow \Xi^0 e^+ \nu_e)$ = $(7 \pm 4)\%$ [1, 98]	CLEO II	$7.18 \pm 0.90_{\text{stat}} \pm 0.98_{\text{syst}}\%$ [90] (LQCD)
		$12.17 \pm 1.35\%$ [101] (SU(3))
		$(11.9 \pm 1.3, 9.8 \pm 1.1, 10.7 \pm 0.9)\%$ [102] (SU(3))
		$11.3 \pm 3.4\%$ [79] (LFQM)
		$10.2 \pm 2.2\%$ [103] (QCDSR)
		$5.20 \pm 1.02\%$ [104] (LFQM)
		$5.39\%$ [108] (LFQM)
		$5.51 \pm 1.65\%$ [106] (LCSR)
		$9.40\%$ [109] (RQM)
$\mathcal{B}(\Omega_c^0 \rightarrow \Omega^- e^+ \nu_e)/\mathcal{B}(\Omega_c^0 \rightarrow \Omega^- \pi^+)$ = $2.4 \pm 1.2$ [1, 99]	CLEO II	$0.71$ [110] (LCSR)
$\mathcal{B}(\Omega_c^0 \rightarrow \Omega^- e^+ \nu_e)/\mathcal{B}(\Omega_c^0 \rightarrow \Omega^- \pi^+)$ = $1.98 \pm 0.13_{\text{stat}} \pm 0.08_{\text{syst}}$ [100]	Belle	$0.9 \pm 0.1$ [91] (LFQM), $0.71$ [110] (LCSR)
$\mathcal{B}(\Omega_c^0 \rightarrow \Omega^- \mu^+ \nu_\mu)/\mathcal{B}(\Omega_c^0 \rightarrow \Omega^- \pi^+)$ = $1.94 \pm 0.18_{\text{stat}} \pm 0.10_{\text{syst}}$ [100]	Belle	$0.9 \pm 0.1$ [91] (LFQM), $0.68$ [110] (LCSR)
$\mathcal{B}(\Omega_c^0 \rightarrow \Omega^- e^+ \nu_e)/\mathcal{B}(\Omega_c^0 \rightarrow \Omega^- \mu^+ \nu_\mu)$ = $1.02 \pm 0.10_{\text{stat}} \pm 0.02_{\text{syst}}$ [100]	Belle	$\approx 1.0$ [80]

2021 review [14]. The third row gives the SM fits assuming unitarity from PDG [1]. These results are also illustrated in Fig. 9. There are some tensions between the leptonic and semileptonic determinations, as well as with the fits assuming unitarity, at the  $1.7\sigma$  level. However, the uncertainties from the leptonic and semileptonic determinations are much larger than the ones from the global fits that impose the unitarity constraint. The test of the second row unitarity is limited by the precision of  $|V_{cs}|$ . Treating the values as uncorrelated and using  $|V_{cb}| = (41.0 \pm 1.4) \times 10^{-3}$  [1], one gets  $|V_{cd}|^2 + |V_{cs}|^2 + |V_{cb}|^2 = 1.015 \pm 0.035$  for the leptonic and  $|V_{cd}|^2 + |V_{cs}|^2 + |V_{cb}|^2 = 1.000 \pm 14$  for the semileptonic

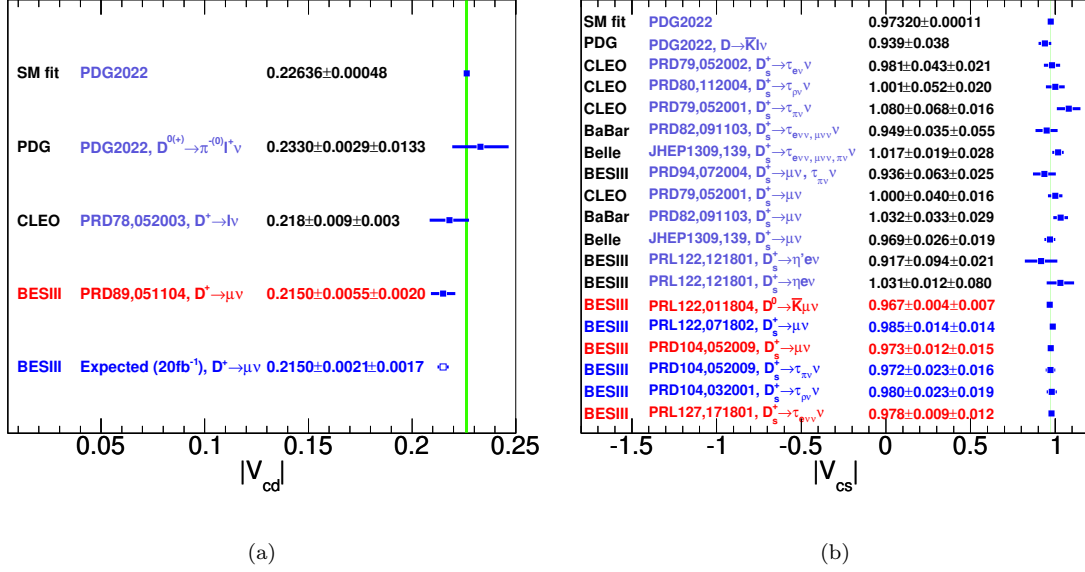


FIG. 8. Precision of the measurements of (a)  $|V_{cd}|$  and (b)  $|V_{cs}|$ . The green bands indicate the uncertainties of the average values from the global fit in SM [1]. (In the case of  $|V_{cs}|$ , the green error band is barely visible, as the SM unitarity constraint leads to very small uncertainty.) The value marked in open square denotes the expected precision with the BESIII data sets that will be accumulated in the future [28]. Data from Refs. [20, 23–26, 32–38, 45, 51]. Figure provided by Hai-Long Ma

determinations. For comparison, the PDG [1] report  $|V_{ud}|^2 + |V_{us}|^2 + |V_{ub}|^2 = 0.9985 \pm 0.0005$  for the test of unitarity of the first row, where the uncertainties are much smaller.

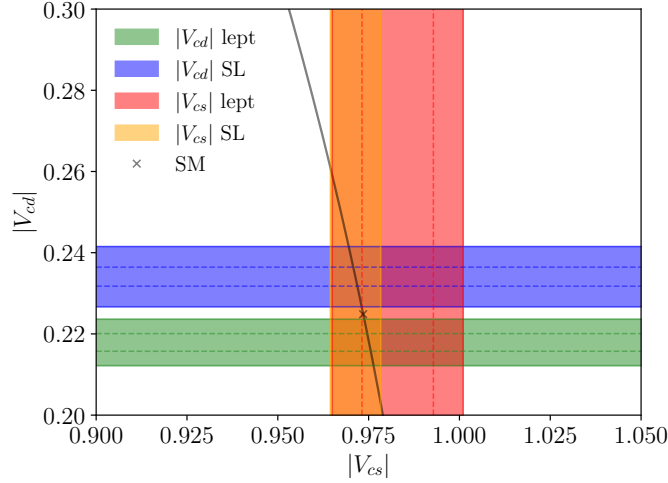


FIG. 9. Summary of the results from leptonic and semileptonic (SL) decays in the  $|V_{cs}|-|V_{cd}|$  plane (see also Eq. (17)). The leptonic and semileptonic determinations are the  $n_f = 2 + 1 + 1$  results from the FLAG 2021 review [14], and the cross labelled SM is the result from SM fits assuming unitarity from PDG [1]. The black line shows the unitarity constraint  $|V_{cd}|^2 + |V_{cs}|^2 = 1 - |V_{cb}|^2$  using  $|V_{cb}| = (41.0 \pm 1.4) \times 10^{-3}$  [1]. The uncertainty on  $|V_{cb}|$  is smaller than the width of the line. The dashed lines show the anticipated 1% uncertainties in the future.

One can also calculate the ratio  $|V_{cd}/V_{cs}|^2 = 0.048 \pm 0.003_{\text{stat}} \pm 0.001_{\text{sys}}$ , with the BESIII results and the FLAG [14] value for  $(f_{D_s^+}/f_{D^+})^{\text{FLAG}} = 1.1783 \pm 0.0016$ . This value deviates from the expectation given by the CKMfitter group [16],  $|V_{cd}/V_{cs}|^2 = 0.05335 \pm 0.00011$ , by  $1.7\sigma$ .

The uncertainties of  $|V_{cd}|$  and  $|V_{cs}|$  measurements are currently dominated by the limited experimental statistics. With the  $\sim 20 \text{ fb}^{-1}$   $\psi(3770)$  data being taken by BESIII [28], it can be expected that the statistical uncertainty will

be comparable to the uncertainty arising from the LQCD calculations of decay constants. The relative uncertainty on the  $|V_{cs}|$  and  $|V_{cd}|$  determinations will both be improved to the 1% level. If the  $|V_{cd}|$  result is the same as its current measured value, the significance of the discrepancy would increase to about the  $4\sigma$  level as shown in Figs. 8(a) and 9.

#### D. Lepton flavor universality

LFU is one of key predictions in the SM and indicates that three generations of leptons share equal coupling to gauge bosons. Specifically, the purely leptonic decay widths of charmed mesons, Eq. (6), is proportional to the lepton mass-squared, which is the consequence of the helicity suppression. Their ratios between different leptons ( $e^+\nu_e : \mu^+\nu_\mu : \tau^+\nu_\tau$ ) depend only on the lepton masses and can be accurately predicted to be  $2.35 \times 10^{-5} : 1 : 2.67$  for  $D^+$  and  $2.35 \times 10^{-5} : 1 : 9.75$  for  $D_s^+$  based on SM with negligible uncertainty (the only uncertainty is coming from the determination of the lepton masses). The  $D_{(s)}^+ \rightarrow e^+\nu_e$  decay, with a  $< 10^{-8}$  expected branching fraction, is not experimentally observed yet, but comparing the obtained branching fractions of  $D_{(s)}^+ \rightarrow \tau^+\nu_\tau$  and  $D_{(s)}^+ \rightarrow \mu^+\nu_\mu$  gives important comprehensive test of  $\tau$ - $\mu$  lepton-flavor universality. Using the world average PDG values [1], one can determine  $\Gamma(D^+ \rightarrow \tau^+\nu_\tau)/\Gamma(D^+ \rightarrow \mu^+\nu_\mu) = 3.21 \pm 0.74$  and  $\Gamma(D_s^+ \rightarrow \tau^+\nu_\tau)/\Gamma(D_s^+ \rightarrow \mu^+\nu_\mu) = 9.80 \pm 0.34$  which, although still statistically limited, are consistent with the SM predictions.

Analogously, the ratios of electronic and muonic semileptonic decay widths of charmed mesons can also be accurately calculated based on Eq. (10), while decays involving  $\omega, \eta, \rho$  receive about 5% uncertainty from the form factor models. These predictions along with the experimental results examine the LFU in the  $e$ - $\mu$  sector. However, suffering from experimental uncertainty of several percent to few ten percent, no significant LFU violation has been observed yet in the charm sector. The best test of  $\mu$ - $e$  LFU for semi-leptonic  $D_{(s)}^{0(+)}$  decays is expected to be from  $D \rightarrow \bar{K}\ell^+\nu_\ell$  decays, where the precision of the test can be reduced from 1.3% to the level of 0.8% with the forthcoming BESIII data. Comparison of the SM prediction of the  $\mu$ - $e$  LFU as a function of  $q^2$  in the  $D \rightarrow \bar{K}\ell\nu_\ell$  decay calculated using LQCD form factors and the current experimental results from BESIII [45] is shown in Fig. 10 (taken from [67]). The figure highlights the fact that the uncertainties from LQCD are negligible compared to experimental uncertainties, and the aforementioned increase in statistics is needed to detect any possible violations in LFU in  $D \rightarrow \bar{K}\ell\nu_\ell, \ell = e, \mu$  decays. At present, it is not conclusive about whether the  $\mu$ - $e$  LFU always holds in semi-leptonic  $D_{(s)}^{0(+)}$  decays, as there are still many un-observed semi-muonic decays, e.g.  $D^+ \rightarrow \eta'\mu^+\nu_\mu, D^{0(+)} \rightarrow a_0(980)\mu^+\nu_\mu, D^{0(+)} \rightarrow K_1(1270)\mu^+\nu_\mu, D^+ \rightarrow f_0(500)\mu^+\nu_\mu, D_s^+ \rightarrow K^0\mu^+\nu_\mu, D_s^+ \rightarrow K^{*0}\mu^+\nu_\mu, D_s^+ \rightarrow f_0(980)\mu^+\nu_\mu,$  and  $D_s^+ \rightarrow \eta'\mu^+\nu_\mu$ . Larger data samples will offer opportunities to search for these decays and thereby clarify if there is possible violation of  $\mu$ - $e$  LFU in the charmed meson sector. For the semi-leptonic charmed baryon decays, there are experimental results of  $\Lambda_c^+ \rightarrow \Lambda\ell^+\nu_\ell$  by BESIII [12, 13](Table II),  $\Omega_c^0 \rightarrow \Omega^-\ell^+\nu_\ell$  and  $\Xi_c^0 \rightarrow \Xi^-\ell^+\nu_\ell$  by Belle [96, 100](Table III), which test the  $\mu$ - $e$  LFU in the charmed baryon sector.

#### E. Rare leptonic and semileptonic $D_{(s)}$ decays

The rare leptonic and semileptonic decays of the  $D_{(s)}$  meson provide a sensitive probe for new physics. In recent years, the Belle, BaBar, LHCb, and BESIII experiments performed many new measurements to search for new physics in this area.

Charm decays with two oppositely charged leptons ( $\ell^+\ell^-$ ) in the final state may proceed via the quark flavor-changing neutral-current (FCNC) process  $c \rightarrow u\ell^+\ell^-$ . FCNC processes are forbidden at tree level in the SM and only allowed in loop and box diagrams, which are highly suppressed by the Glashow-Iliopoulos-Maiani (GIM) mechanism. Therefore, they provide a unique opportunity to search contributions from new physics beyond the SM via couplings to up-type quarks. The expected branching fractions of the FCNC decays  $D^0 \rightarrow e^+e^-$  and  $D^0 \rightarrow \mu^+\mu^-$  in the SM are at  $\mathcal{O}(10^{-13})$ . Nowadays the sensitivity of experimental measurements for the branching fractions has reach  $10^{-9}$  [111–114], but no evidence is observed yet. The GIM suppression is more effective for the charm sector compared to the down-type quarks in the bottom and strange sectors. This suppression is responsible for the relatively small size of charm mixing and CP violation in the charm system. Therefore, FCNC processes in  $D \rightarrow h\ell^+\ell^-$  decays are often totally overshadowed by long distance contributions, where  $h$  denotes one or more hadrons. The short-distance

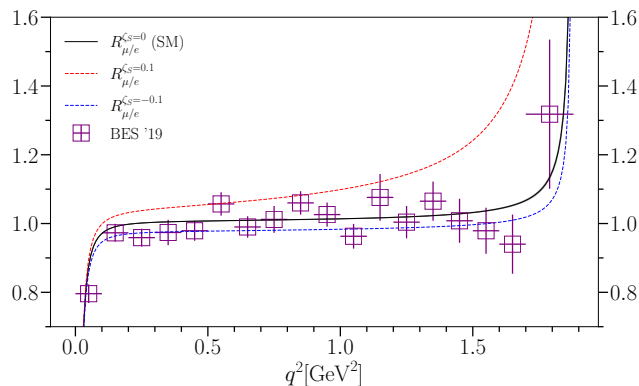


FIG. 10. Lepton flavour universality tests in  $D \rightarrow \bar{K} \ell \nu_\ell$  decay. The solid black curve as a function of  $q^2$  shows the SM ratio of branching fractions for a muon in the final state to that for an electron obtained from LQCD form factors (for details see Ref. [67] where this plot is from). The width of the curve gives the (very small) uncertainty from LQCD. Possible QED effects are not included. The points, with error bars, are from the BESIII experiment [45]. The red and blue dashed lines show what the curve would look like in the presence of a new physics scalar coupling for the  $\mu$  case (for details see Ref. [67]). Figure from Ref. [67].

contributions from FCNC to the branching fraction of  $D \rightarrow h \ell^+ \ell^-$  are expected to the order of  $\mathcal{O}(10^{-9})$ , while long-distance contributions from tree-level processes involving intermediate vector resonances, i.e.  $D \rightarrow h V (\rightarrow \ell^+ \ell^-)$ , are predicted to increase the branching fraction to  $\mathcal{O}(10^{-6})$ . Many relevant attempts have been made to impose constraints on physics beyond the SM [115–126].

Decay modes with two oppositely charged leptons of different flavor correspond to lepton flavor violating (LFV) decays and are essentially forbidden in the SM because they can occur only through lepton mixing. Decays involving two same-sign leptons are both LFV and lepton-number violating (LNV) decays, which is also strictly suppressed in the SM. An interesting source of LNV processes is given by exchanging a single Majorana neutrino with a mass on the order of the heavy flavor mass scale, where the Majorana neutrino can be kinematically accessible and produced on shell. Although no significant signal is observed so far, the experimental results provide the supplementary information in the study of lepton-mixing and the nature of neutrinos [112, 113, 115, 118, 125, 127–129].

## VII. DISCUSSION AND OUTLOOK

The SM is the greatest successful theoretical framework of particle physics, but there are still a number of issues that deserve further both experimental and theoretical investigation. Purely leptonic and semileptonic decays of charmed hadrons remain the best platform to test the SM in the charm sector. In this review, we have summarized the recent results obtained in the BESIII experiments with data sets collected at the production thresholds of  $D\bar{D}$ ,  $D_s^{*+} D_s^-$  and  $\Lambda_c^+ \bar{\Lambda}_c^-$ , and review the theoretical and experimental tools used. We have also summarized the updated measurements of semileptonic  $\Xi_c^{0,+}$  and  $\Omega_c$  decays by Belle, CLEO II, and ALICE experiments. These unique opportunities provide rigorous tests of QCD-based models, the unitarity of CKM matrix, and leptonic-flavor universality in the charm energy region.

Our knowledge of hadronic charm purely leptonic and semileptonic decays has improved significantly over the last few years. The values of the decay constants and form factors can be calculated in high precision from first principles using LQCD. The obtained precision for the  $f_{D_{(s)}^+}$  calculations has reached the 0.2–0.3% level, and can translate leptonic decay rate measurements into high precision determinations of the CKM matrix elements  $|V_{cd}|$  and  $|V_{cs}|$ . Moreover, the highly accurate prediction of  $f_{D_{(s)}^+}$  and form factors by LQCD allow detailed theoretical studies of the charmed hadron decay dynamics, such as SU(3). However, the current experimental results can only provide relative low-precision calibration or tests of theoretical model calculations with limited amount of data samples.

The data samples at the  $D\bar{D}$  and  $D_s^{*+} D_s^-$  thresholds to be collected by BESIII in the coming years offer opportunities

to further improve the precision of the measurements of these important constants. The relative uncertainties on  $|V_{cd}|f_{D^+}$  and  $|V_{cs}|f_{D_s^+}$  can be reduced from 2.6% and 1.2% to approximately 1.1% and 0.9%, respectively, and the systematic uncertainty is expected to dominate at that time. As the leptonic determinations of the CKM matrix elements have uncertainties that are reaching the percent level, higher-order electroweak and hadronic-structure dependent corrections to the decay rate become important. These have not been computed for  $D_{(s)}$  meson decays yet, but for pion and kaon decays they have been estimated to be around 1–2% [130]. It is therefore important that such theoretical calculations are tackled in the near future. The uncertainties of lepton-flavor universality tests in  $D^+ \rightarrow \ell^+ \nu_\ell$  and  $D_s^+ \rightarrow \ell^+ \nu_\ell$  decays are also expected to be reduced from 24.0% and 4.0% to about 10.0% and 3.0%, respectively.

The precision of all measurements of semi-leptonic  $D_{(s)}^{0(+)} \rightarrow P$  and  $D_{(s)}^{0(+)} \rightarrow V$  form factors, except for the  $D^{0(+)} \rightarrow K$  and  $D^{0(+)} \rightarrow K^*$ , are restricted due to limited data sets. With BESIII future data samples, all the form-factor measurements which are currently statistically limited will be statistically improved by a factor of up to 2.6 and 1.4 for semi-leptonic  $D^{0(+)}$  and  $D_s^+$  decays, respectively. The dynamics studies of the semi-leptonic  $D \rightarrow P$  decays will offer complementary measurements of  $|V_{cs}|$  and  $|V_{cd}|$  using the whole kinematic  $q^2$  range. The current precisions of the  $|V_{cd}|$  measurements with semileptonic  $D^{0(+)}$  decays are limited by the theoretical uncertainties of the form factors in LQCD, with FLAG quoting a 4.4% uncertainty for  $f_+^{D \rightarrow \pi}(0)$  from  $n_f = 2 + 1$  calculations and 5.7% from  $n_f = 2 + 1 + 1$  calculations [14]. Here the situation can be expected to improve within the next year or two, as two collaborations are finalising their ongoing calculations [74, 75]<sup>4</sup>, and the determination of  $V_{cd}$  from semileptonic decays with  $\sim 1\%$  uncertainties should become possible. For  $|V_{cs}|$  the situation is much better, as lattice calculations have reached below 1% precision for the form factors of  $D \rightarrow \bar{K} \ell \nu_\ell$  decays, thus allowing the extraction of  $|V_{cs}|$  at similar precision (FLAG [14] quote a 0.7% uncertainty from their fit). At this precision, incorporation of electromagnetic corrections from first principles is a necessary step in the near future. In addition, the forthcoming BESIII data will allow to extract the  $D \rightarrow S$  and  $D \rightarrow A$  form factors from experiment for the first time.

Charmed hadron studies will continue during the future upgrade of the BESIII experiment. BESIII plans to collect 7 times the current amount of  $D\bar{D}$  threshold data, and this will usher in a precision charm flavor era. Along with the improvements in the LQCD calculations on the decay constants and form factors expected circa 2025, we can then anticipate significantly improved constraints on the  $(|V_{cs}|, |V_{cd}|)$  plane [28]. This will allow for precise tests of the consistency of CKM determinations from different quark sectors [28, 132].

Following BESIII, the Super Tau-Charm Facility (STCF) [5] has been proposed in China, which is a symmetric electron-positron collider operating at  $\sqrt{s}$  from 2.0 to 7.0 GeV. The energy region of STCF covers the pair production thresholds for  $D^{0(+)}$ ,  $D_s^+$ ,  $\Lambda_c^+$ ,  $\Xi_c^{0(+)}$  and  $\Omega_c^0$  hadrons. The peak luminosity is designed to be over  $0.5 \times 10^{35} \text{ cm}^{-2} \text{ s}^{-1}$  at 4.0 GeV and the designed integrated luminosity per year is approximate  $1 \text{ ab}^{-1}$ , corresponding to a data rate about a factor 100 larger than the present BEPCII. The STCF will become a precision frontier for exploring the nature of non-perturbative strong interactions, understanding the internal structure of hadrons, studying the CP violation of hadron decays and searching for the asymmetry of matter-antimatter, and testing the SM and probing for physics beyond the SM with unprecedented sensitivity.

## ACKNOWLEDGMENTS

This work is supported in part by National Key R&D Program of China under Contracts Nos. 2020YFA0406300, 2020YFA0406400; National Natural Science Foundation of China (NSFC) under Contracts Nos. 11935018, 11875054, 12192263, 11935015, 12221005; the Chinese Academy of Sciences (CAS) Large-Scale Scientific Facility Program; Joint Large-Scale Scientific Facility Funds of the NSFC and CAS under Contracts No. U2032104; J.K. acknowledges support by the European Research Council (ERC) under the European Union's Horizon 2020 research and innovation program

---

<sup>4</sup> We note that a new paper by Fermilab Lattice and MILC collaborations has appeared in the arXiv [131], after this review article had already been submitted to ARNP.

through Grant Agreement No. 771971-SIMDAMA.

- 
- [1] R. L. Workman et al. *Prog. Theor. Exp. Phys.*, 2022:083C01, 2022.
  - [2] M. Kobayashi and T. Maskawa. *Progress of Theoretical Physics*, 49(2):652–657, 02 1973.
  - [3] Ling-Lie Chau and Wai-Yee Keung. Comments on the Parametrization of the Kobayashi-Maskawa Matrix. *Phys. Rev. Lett.*, 53:1802, 1984.
  - [4] M. N. Achasov et al. *Snowmass 2021*, [https://www.snowmass21.org/docs/files/summaries/RF/SNOWMASS21-RF1\\_RF7\\_BINP-019.pdf](https://www.snowmass21.org/docs/files/summaries/RF/SNOWMASS21-RF1_RF7_BINP-019.pdf), 2021.
  - [5] J. B. Liu et al. *Snowmass 2021*, [https://www.snowmass21.org/docs/files/summaries/RF/SNOWMASS21-RF7\\_RF1\\_STCF-013.pdf](https://www.snowmass21.org/docs/files/summaries/RF/SNOWMASS21-RF7_RF1_STCF-013.pdf), 2021.
  - [6] Marco Gersabeck. *PoS*, FWNP:001, 2015.
  - [7] A. J. Bevan et al. *Eur. Phys. J. C*, 74:3026, 2014.
  - [8] M. Ablikim et al. *Phys. Lett. B*, 603:130–137, 2004.
  - [9] LHCb collaboration. *LHCb-CONF-2010-013*, Dec, 2010.
  - [10] H. Albrecht et al. *Phys. Lett. B*, 269:234–242, 1991.
  - [11] T. Bergfeld et al. *Phys. Lett. B*, 323:219–226, 1994.
  - [12] M. Ablikim et al. *Phys. Rev. Lett.*, page Accepted, 2022. arXiv:2207.14149.
  - [13] M. Ablikim et al. *Physics Letters B*, 767:42–47, 2017.
  - [14] Y. Aoki et al. *Eur. Phys. J. C*, 82(10):869, 2022.
  - [15] D. Silverman and H. Yao. *Phys. Rev. D*, 38:214–232, Jul 1988.
  - [16] J. Charles et al. *Eur. Phys. J. C*, 41(1):1–131, 2005. [updated results and plots available at: <http://ckmfitter.in2p3.fr>].
  - [17] A. Bazavov et al. *Phys. Rev. D*, 85:114506, 2012.
  - [18] A. Bazavov et al. *Phys. Rev. D*, 90(7):074509, 2014.
  - [19] A. Bazavov et al. *Phys. Rev. D*, 98(7):074512, 2018.
  - [20] M. Ablikim et al. *Phys. Rev. D*, 89(5):051104, 2014.
  - [21] N. Carrasco et al. *Phys. Rev. D*, 91(5):054507, 2015.
  - [22] M. Ablikim et al. *Phys. Rev. Lett.*, 123(21):211802, 2019.
  - [23] M. Ablikim et al. *Phys. Rev. D*, 104(5):052009, 2021.
  - [24] M. Ablikim et al. *Phys. Rev. D*, 104(3):032001, 2021.
  - [25] M. Ablikim et al. *Phys. Rev. Lett.*, 127(17):171801, 2021.
  - [26] M. Ablikim et al. *Phys. Rev. Lett.*, 122(7):071802, 2019.
  - [27] Y. Amhis et al. Heavy Flavor Averaging Group (HFLAV) 2022, arXiv:2206.07501.
  - [28] M. Ablikim et al. *Chin. Phys. C*, 44(4):040001, 2020.
  - [29] P. A. Boyle, L. Del Debbio, A. Jüttner, A. Khamsheh, F. Sanfilippo, and J. T. Tsang. *JHEP*, 12:008, 2017.
  - [30] Y. B. Yang et al. *Phys. Rev. D*, 92(3):034517, 2015.
  - [31] C. T. H. Davies, C. McNeile, E. Follana, G. P. Lepage, H. Na, and J. Shigemitsu. *Phys. Rev. D*, 82:114504, 2010.
  - [32] P. U. E. Onyisi et al. *Phys. Rev. D*, 79:052002, 2009.
  - [33] P. Naik et al. *Phys. Rev. D*, 80:112004, 2009.
  - [34] J. P. Alexander et al. *Phys. Rev. D*, 79:052001, 2009.
  - [35] P. del Amo Sanchez et al. *Phys. Rev. D*, 82:091103, 2010. [Erratum: *Phys.Rev.D* 91, 019901 (2015)].
  - [36] A. Zupanc et al. *JHEP*, 09:139, 2013.
  - [37] M. Ablikim et al. *Phys. Rev. D*, 94(7):072004, 2016.
  - [38] B. I. Eisenstein et al. *Phys. Rev. D*, 78:052003, 2008.
  - [39] M. A. Ivanov, J. G. Körner, J. N. Pandya, P. Santorelli, N. R. Soni, and C. T. Tran. *Front. Phys. (Beijing)*, 14(6):64401, 2019.
  - [40] M. Ablikim et al. *Phys. Rev. D*, 92(7):072012, 2015.
  - [41] M. Ablikim et al. *Phys. Rev. D*, 96(1):012002, 2017.
  - [42] M. Ablikim et al. *Phys. Rev. D*, 92(11):112008, 2015.
  - [43] M. Ablikim et al. *Phys. Rev. D*, 104(5):052008, 2021.
  - [44] M. Ablikim et al. *Chin. Phys. C*, 40(11):113001, 2016.
  - [45] M. Ablikim et al. *Phys. Rev. Lett.*, 122(1):011804, 2019.
  - [46] M. Ablikim et al. *Eur. Phys. J. C*, 76(7):369, 2016.
  - [47] M. Ablikim et al. *Phys. Rev. Lett.*, 122(6):061801, 2019.
  - [48] M. Ablikim et al. *Phys. Rev. Lett.*, 121(17):171803, 2018.
  - [49] M. Ablikim et al. *Phys. Rev. D*, 97(9):092009, 2018.
  - [50] M. Ablikim et al. *Phys. Rev. Lett.*, 124(23):231801, 2020.
  - [51] M. Ablikim et al. *Phys. Rev. Lett.*, 122(12):121801, 2019.
  - [52] M. Ablikim et al. *Phys. Rev. D*, 94(11):112003, 2016.
  - [53] M. Ablikim et al. *Phys. Rev. D*, 97(1):012006, 2018.

- [54] M. Ablikim et al. *Phys. Rev. D*, 94(3):032001, 2016.
- [55] M. Ablikim et al. *Phys. Rev. D*, 99(1):011103, 2019.
- [56] M. Ablikim et al. *Phys. Rev. Lett.*, 122(6):062001, 2019.
- [57] M. Ablikim et al. *Phys. Rev. D*, 104(9):L091103, 2021.
- [58] M. Ablikim et al. *Phys. Rev. D*, 92(7):071101, 2015.
- [59] M. Ablikim et al. *Phys. Rev. D*, 101(7):072005, 2020.
- [60] M. Ablikim et al. *Phys. Rev. D*, 105(3):L031101, 2022.
- [61] M. Ablikim et al. *Phys. Rev. Lett.*, 121(8):081802, 2018.
- [62] M. Ablikim et al. *Phys. Rev. D*, 103(9):092004, 2021.
- [63] M. Ablikim et al. *Phys. Rev. Lett.*, 123(23):231801, 2019.
- [64] M. Ablikim et al. *Phys. Rev. Lett.*, 127(13):131801, 2021.
- [65] M. Ablikim et al. *Phys. Rev. D*, 102(11):112005, 2020.
- [66] H. Na, C. T. H. Davies, E. Follana, J. Koponen, G. P. Lepage, and J. Shigemitsu. *Phys. Rev. D*, 84:114505, 2011.
- [67] B. Chakraborty, W. G. Parrott, C. Bouchard, C. T. H. Davies, J. Koponen, and G. P. Lepage. *Phys. Rev. D*, 104(3):034505, 2021.
- [68] V. Lubicz, L. Riggio, G. Salerno, S. Simula, and C. Tarantino. *Phys. Rev. D*, 96(5):054514, 2017. [Erratum: *Phys.Rev.D* 99, 099902 (2019), Erratum: *Phys.Rev.D* 100, 079901 (2019)].
- [69] V. Lubicz, L. Riggio, G. Salerno, S. Simula, and C. Tarantino. *Phys. Rev. D*, 96(5):054514, 2017. [Erratum: *Phys.Rev.D* 99, 099902 (2019), Erratum: *Phys.Rev.D* 100, 079901 (2019)].
- [70] L. Widhalm et al. *Phys. Rev. Lett.*, 97:061804, 2006.
- [71] B. Aubert et al. *Phys. Rev. D*, 76:052005, 2007.
- [72] D. Besson et al. *Phys. Rev. D*, 80:032005, 2009.
- [73] S. Meinel. *Phys. Rev. Lett.*, 118(8):082001, 2017.
- [74] M. Marshall, P. Boyle, L. Del Debbio, F. Erben, J. Flynn, A. Jüttner, A. Portelli, J. T. Tsang, and O. Witzel. *PoS, LATTICE2021:416*, 2022.
- [75] W. I. Jay, A. Lytle, C. DeTar, A. X. El-Khadra, E. Gamiz, Z. Gelzer, S. Gottlieb, A. Kronfeld, J. Simone, and A. Vaquero. *PoS, LATTICE2021:109*, 2022.
- [76] J. Koponen. In *6th International Workshop on Charm Physics*, 11 2013.
- [77] J. Koponen. In *8th International Workshop on the CKM Unitarity Triangle*, 11 2014.
- [78] P. Ball. *Phys. Lett. B*, 641:50–56, 2006.
- [79] C. Q. Geng, C. W. Liu, and T. H. Tsai. *Phys. Rev. D*, 103(5):054018, 2021.
- [80] F. Huang and Q. A. Zhang. *Eur. Phys. J. C*, 82(1):11, 2022.
- [81] Y. Amhis et al. *Eur. Phys. J. C*, 77(12):895, 2017.
- [82] C. Bourrely, I. Caprini, and L. Lellouch. *Phys. Rev. D*, 79:013008, 2009. [Erratum: *Phys.Rev.D* 82, 099902 (2010)].
- [83] L. Riggio, G. Salerno, and S. Simula. *Eur. Phys. J. C*, 78(6):501, 2018.
- [84] J. P. Lees et al. *Phys. Rev. D*, 91(5):052022, 2015.
- [85] B. Aubert et al. *Phys. Rev. D*, 78:051101, 2008.
- [86] G. C. Donald, C. T. H. Davies, J. Koponen, and G. P. Lepage. *Phys. Rev. D*, 90(7):074506, 2014.
- [87] M. Ablikim et al. *Phys. Rev. Lett.*, 115:221805, Nov 2015.
- [88] M. Ablikim et al. 7 2022. arXiv:2207.11483.
- [89] S. Meinel. *Phys. Rev. D*, 97(3):034511, 2018.
- [90] Q. A. Zhang et al. *Chin. Phys. C*, 46(1):011002, 2022.
- [91] Y. K. Hsiao, L. Yang, C. C. Lih, and S. T. Tsai. *Eur. Phys. J. C*, 80(11):1066, 2020.
- [92] Q. P. Xu and A. N. Kamal. *Phys. Rev. D*, 46:3836–3844, 1992.
- [93] H. Y. Cheng. *Phys. Rev. D*, 56:2799–2811, 1997. [Erratum: *Phys.Rev.D* 99, 079901 (2019)].
- [94] T. Gutsche, M. A. Ivanov, J. G. Körner, and V. E. Lyubovitskij. *Phys. Rev. D*, 98(7):074011, 2018.
- [95] M. Pervin, W. Roberts, and S. Capstick. *Phys. Rev. C*, 74:025205, 2006.
- [96] Y. B. Li et al. *Phys. Rev. Lett.*, 127(12):121803, 2021.
- [97] S. Acharya et al. *Phys. Rev. Lett.*, 127(27):272001, 2021.
- [98] J. P. Alexander et al. *Phys. Rev. Lett.*, 74:3113–3117, 1995. [Erratum: *Phys.Rev.Lett.* 75, 4155 (1995)].
- [99] R. Ammar et al. *Phys. Rev. Lett.*, 89:171803, 2002.
- [100] Y. B. Li et al. *Phys. Rev. D*, 105(9):L091101, 2022.
- [101] X. G. He, F. Huang, W. Wang, and Z. P. Xing. *Phys. Lett. B*, 823:136765, 2021.
- [102] C. Q. Geng, C. W. Liu, T. H. Tsai, and S. W. Yeh. *Phys. Lett. B*, 792:214–218, 2019.
- [103] Z. X. Zhao. 3 2021.
- [104] H. W. Ke, Q. Q. Kang, X. H. Liu, and Xue-Qian Li. *Chin. Phys. C*, 45(11):113103, 2021.
- [105] K. Azizi, Y. Sarac, and H. Sundu. *Eur. Phys. J. A*, 48:2, 2012.
- [106] T. M. Aliev, S. Bilmis, and M. Savci. *Phys. Rev. D*, 104(5):054030, 2021.
- [107] H. H. Duan, Y. L. Liu, and M. Q. Huang. 1 2022.
- [108] Z. X. Zhao. *Chin. Phys. C*, 42(9):093101, 2018.
- [109] R. N. Faustov and V. O. Galkin. *Eur. Phys. J. C*, 79(8):695, 2019.
- [110] T. M. Aliev, M. Savci, and S. Bilmis. *Phys. Rev. D*, 106(7):074022, 2022.
- [111] B. Aubert et al. *Phys. Rev. Lett.*, 93:191801, 2004.
- [112] M. Petric et al. *Phys. Rev. D*, 81:091102, 2010.

- [113] J. P. Lees et al. *Phys. Rev. D*, 86:032001, 2012.
- [114] R. Aaij et al. *Phys. Lett. B*, 725:15–24, 2013.
- [115] J. P. Lees et al. *Phys. Rev. D*, 84:072006, 2011.
- [116] R. Aaij et al. *Phys. Lett. B*, 724:203–212, 2013.
- [117] R. Aaij et al. *Phys. Rev. D*, 97(9):091101, 2018.
- [118] R. Aaij et al. *J. High Energ. Phys.*, 2021:44, Jun 2021.
- [119] M. Ablikim et al. *Phys. Rev. D*, 105:L071102, Apr 2022.
- [120] R. Aaij et al. *Phys. Lett. B*, 728:234–243, 2014.
- [121] R. Aaij et al. *Physics Letters B*, 757:558–567, 2016.
- [122] R. Aaij et al. *Phys. Rev. Lett.*, 119(18):181805, 2017.
- [123] R. Aaij et al. *Phys. Rev. Lett.*, 121(9):091801, 2018.
- [124] J. P. Lees et al. *Phys. Rev. Lett.*, 122:081802, Feb 2019.
- [125] J. P. Lees et al. *Phys. Rev. Lett.*, 124(7):071802, 2020.
- [126] R. Aaij et al. *Phys. Rev. Lett.*, 128:221801, Jun 2022.
- [127] R. Aaij et al. *Phys. Lett. B*, 754:167–175, 2016.
- [128] J. P. Lees et al. *Phys. Rev. D*, 101(11):112003, 2020.
- [129] M. Ablikim et al. *Phys. Rev. D*, 99(11):112002, 2019.
- [130] V. Cirigliano and I. Rosell. *JHEP*, 10:005, 2007.
- [131] Alexei Bazavov et al. 2022. arXiv:2212.12648.
- [132] J. Charles, A. Hocker, H. Lacker, S. Laplace, F. R. Le Diberder, J. Malcles, J. Ocariz, M. Pivk, and L. Roos. *Eur. Phys. J. C*, 41(1):1–131, 2005.